# Charge Separation in a Novel Artificial Photosynthetic Reaction Center Lives 380 ms

**Hiroshi Imahori,* Dirk M. Guldi,*,† Koichi Tamaki,‡ Yutaka Yoshida, Chuping Luo,† Yoshiteru Sakata,‡ and Shunichi Fukuzumi***

*Contribution from the Department of Material and Life Science, Graduate School of Engineering, Osaka University, CREST, Japan Science and Technology Corporation, Suita, Osaka 565-0871, Japan, Radiation Laboratory, University of Notre Dame, Notre Dame, Indiana 46556, and The Institute of Scientific and Industrial Research, Osaka University, 8-1 Mihoga-oka, Ibaraki, Osaka 567-0047, Japan.*

*Received November 30, 2000. Revised Manuscript Received May 2, 2001*

**Abstract:** An extremely long-lived charge-separated state has been achieved successfully using a ferrocene−zincporphyrin−freebaseporphyrin−fullerene tetrad which reveals a cascade of photoinduced energy transfer and multistep electron transfer within a molecule in frozen media as well as in solutions. The lifetime of the resulting charge-separated state (i.e., ferricenium ion−$C_{60}$ radical anion pair) in a frozen benzonitrile is determined as 0.38 s, which is more than one order of magnitude longer than any other *intramolecular* charge recombination processes of synthetic systems, and is comparable to that observed for the bacterial photosynthetic reaction center**.** Such an extremely long lifetime of the tetrad system has been well correlated with the charge-separated lifetimes of two homologous series of porphyrin−fullerene dyad and triad systems.

Electron transfer (ET) chemistry in biological and artificial systems has been among the most intensively studied topics over the past decades.[1−10] Natural photosynthesis applies ET systems, where a relay of ET reactions evolves among chlorophyll and quinone moieties embedded in a transmembrane protein matrix. Ultimately the product of this cascade is conversion of light into usable chemical energy.[11] The mimicry of these complex and highly versatile processes has prompted the design of synthetic donor−acceptor linked ensembles such as triads, tetrads, and pentads.[6−10] However, achieving the long lifetime and the high efficiency of charge separation (CS) like natural photosynthesis has been mainly hampered by synthetic difficulties. A specific challenge involves attaining a fine-tuned and directed redox gradient along donor−acceptor linked arrays.

With the advent of fullerenes, a new three-dimensional electron acceptor became available, exhibiting attractive characteristics.[12] In particular, fullerenes have remarkably small reorganization energies of ET, which result from the $\pi$ electron systems delocalized over the three-dimensional surface together

* Author to whom correspondence should be addressed. E-mail: imahori@ap.chem.eng.osaka-u.ac.jp; guldi.1@nd.edu; fukuzumi@ap.chem.eng.osaka-u.ac.jp.

† University of Notre Dame.

‡ The Institute of Scientific and Industrial Research, Osaka University.

(1) (a) Marcus, R. A.; Sutin, N. *Biochim. Biophys. Acta* **1985**, *811*, 265. (b) Marcus, R. A. *Angew. Chem., Int. Ed. Engl.* **1993**, *32*, 1111. (c) Bixon, M.; Jortner, J. In *Electron Transfer−From Isolated Molecules to Biomolecules*; Bixon, M., Jortner, J., Eds.; John Wiley & Sons: New York, 1999; Part 1, pp 35−202. (d) Newton, M. D. *Chem. Rev.* **1991**, *91*, 767.

(2) (a) Beratan, D. N.; Betts, J. N.; Onuchic, J. N. *Science* **1991**, *252*, 1285. (b) Winkler, J. R.; Gray, H. B. *Chem. Rev.* **1992**, *92*, 369. (c) Moser, C. C.; Keske, J. M.; Warncke, K.; Farid, R. S.; Dutton, P. L. *Nature* **1992**, *355*, 796. (d) Kirmaier, C.; Holton, D. In *The Photosynthetic Reaction Center*; Deisenhofer, J., Norris, J. R., Eds.; Academic Press: San Diego, 1993; Vol. II, pp 49−70. (e) Langen, R.; Chang, I.-J.; Germanas, J. P.; Richards, J. H.; Winkler, J. R.; Gray, H. B. *Science* **1995**, *268*, 1733. (f) Page, C. C.; Moser, C. C.; Chen, X.; Dutton, P. L. *Nature* **1999**, *402*, 47.

(3) (a) Willner, I. *Acc. Chem. Res.* **1997**, *30*, 347. (b) Willner, I.; Willner, B. In *Advances in Photochemistry*; Neckers, D. C., Volman, D. H., Von Bünau, G., Eds.; Wiley: London, 1995; Vol. 20, p 217. (c) McLendon, G.; Hake, R. *Chem. Rev.* **1992**, *92*, 481. (d) Lewis, F. D.; Letsinger, R. L.; Wasielewski, M. R. *Acc. Chem. Res.* **2001**, *34*, 159.

(4) (a) Gould, I. R.; Farid, S. *Acc. Chem. Res.* **1996**, *29*, 522. (b) Mataga, N.; Miyasaka, H. In *Electron Transfer-From Isolated Molecules to Biomolecules*; Jortner, J., Bixon, M., Eds.; John Wiley & Sons: New York, 1999; Part 2, pp 431−496.

(5) (a) Miller, J. R.; Calcaterra, L. T.; Closs, G. L. *J. Am. Chem. Soc.* **1984**, *106*, 3047. (b) Closs, G. L.; Miller, J. R. *Science* **1988**, *240*, 440. (c) Barbara, P. F.; Meyer, T. J.; Ratner, M. A. *J. Phys. Chem.* **1996**, *100*, 13148.

(6) (a) Connolly, J. S.; Bolton, J. R. In *Photoinduced Electron Transfer*; Fox, M. A., Chanon, M., Eds.; Elsevier: Amsterdam, 1988; Part D, pp 303−393. (b) Wasielewski, M. R. In *Photoinduced Electron Transfer*; Fox, M. A., Chanon, M., Eds.; Elsevier: Amsterdam, 1988; Part A, pp 161−206.

(7) (a) Wasielewski, M. R. *Chem. Rev.* **1992**, *92*, 435. (b) Bixon, M.; Fajer, J.; Feher, G.; Freed, J. H.; Gamliel, D.; Hoff, A. J.; Levanon, H.; Möbius, D.; Norris, J. R.; Nechushtai, R.; Scherz, A.; Sessler, J. L.; Stehlik, D. H. A. *Isr. J. Chem.* **1992**, *32*, 369. (c) Gust, D.; Moore, T. A.; Moore, A. L. *Acc. Chem. Res.* **1993**, *26*, 198. (d) Kurreck, H.; Huber, M. *Angew. Chem., Int. Ed. Engl.* **1995**, *34*, 849. (e) Gust, D.; Moore, T. A. In *The Porphyrin Handbook*; Kadish, K. M., Smith, K. M., Guilard, R., Eds.; Academic Press: San Diego, CA, 2000; Vol. 8, pp 153−190. (f) Gust, D.; Moore, T. A.; Moore, A. L. *Acc. Chem. Res.* **2001**, *34*, 40.

(8) (a) Chambron, J.-C.; Chardon-Noblat, S.; Harriman, A.; Heitz, V.; Sauvage, J.-P. *Pure Appl. Chem.* **1993**, *65*, 2343. (b) Harriman, A.; Sauvage, J.-P. *Chem. Soc. Rev.* **1996**, *26*, 41. (c) Blanco, M.-J.; Jiménez, M. C.; Chambron, J.-C.; Heitz, V.; Linke, M.; Sauvage, J.-P. *Chem. Soc. Rev.* **1999**, *28*, 293. (d) Balzani, V.; Juris, A.; Venturi, M.; Campagna, S.; Serroni, S. *Chem. Rev.* **1996**, *96*, 759. (e) *Electron Transfer in Chemistry*; Balzani, V., Ed.; Wiley-VCH: Weinheim, 2001.

(9) (a) Paddon-Row, M. N. *Acc. Chem. Res.* **1994**, *27*, 18. (b) Verhoeven, J. W. In *Electron Transfer−From Isolated Molecules to Biomolecules*; Jortner, J., Bixon, M., Eds.; John Wiley & Sons: New York, 1999; Part 1, pp 603−644. (c) Maruyama, K.; Osuka, A. *Pure Appl. Chem.* **1990**, *62*, 1511. (d) Maruyama, K.; Osuka, A.; Mataga, N. *Pure Appl. Chem.* **1994**, *66*, 867. (e) Osuka, A.; Mataga, N.; Okada, T. *Pure Appl. Chem.* **1997**, *69*, 797. (f) Sun, L.; Hammarström, L.; Åkermark, B.; Styring, S. *Chem. Soc. Rev.* **2001**, *30*, 36.

(10) (a) Imahori, H.; Sakata, Y. *Adv. Mater.* **1997**, *9*, 537. (b) Imahori, H.; Sakata, Y. *Eur. J. Org. Chem.* **1999**, 2445. (c) Guldi, D. M. *Chem. Commun.* **2000**, 321. (d) Guldi, D. M.; Prato, M. *Acc. Chem. Res.* **2000**, *33*, 695.

(11) (a) *The Photosynthetic Reaction Center*; Deisenhofer, J., Norris, J. R., Eds.; Academic Press: San Diego, 1993. (b) *Anoxygenic Photosynthetic Bacteria*; Blankenship, R. E., Madigan, M. T., Bauer, C. E., Eds.; Kluwer Academic Publishing: Dordrecht, The Netherlands, 1995.

10.1021/ja004123v CCC: $20.00 
Published on Web 06/13/2001

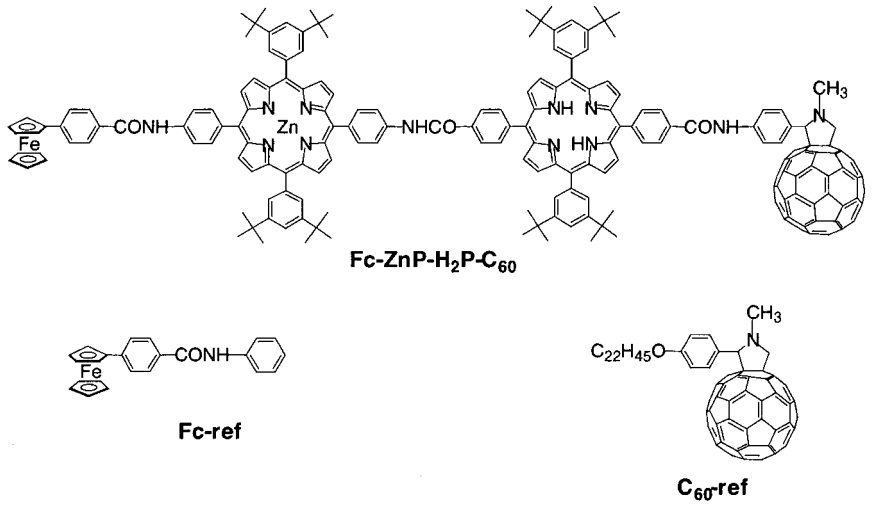


**Figure 1.** Structures of porphyrin−fullerene linked tetrad and the reference compounds.

with the rigid, confined structure of the aromatic $\pi$ sphere.[10,13,14] In this regard, it has been observed frequently that photoinduced CS is accelerated and charge recombination (CR) is decelerated in donor-linked fullerenes, as compared to those with conventional acceptors such as quinones and imides.[10,13] The primary ET processes of the photosynthesis, on the other hand, are also characterized by an extremely small reorganization energy ($\lambda$ = ~0.2 eV). This is essential to achieve the ultrafast forward ET and to retard the energy-wasting back ET, which is highly exergonic ($-\Delta G^0_{BET}$ = 1.1 eV) and thereby deeply in the Marcus inverted region.[11] Taking these facts into concert, a significant impact, concerning the lifetime of CS, is expected without, however, lowering the overall efficiency of CS in fullerene-containing multicomponent systems. Along this line we and others have prepared a variety of donor−fullerene linked dyads and triads,[10,15−23] some of which have successfully mimicked photosynthetic ET on electrodes[23] as well as in solutions.

In this work we wish to report the longest lifetime of a charge-separated state ever achieved in any other artificial reaction center. In particular, in a newly designed ferrocene (Fc)−zincporphyrin (ZnP)−freebaseporphyrin ($H_2P$)-$C_{60}$ tetrad (**Fc-ZnP-$H_2$P-$C_{60}$**; Figure 1) a cascade of photoinduced energy transfer (EN), coupled to a multistep ET, occurs in frozen as well as in condensed liquid media. The lifetime of the resulting charge-separated state (i.e., ferricenium ion ($Fc^+$)−$C_{60}$ radical anion ($C_{60}^{\bullet-}$) pair), as determined in a frozen benzonitrile (PhCN) matrix, amounts to a remarkable 0.38 s. This value is not only more than one-order of magnitude larger than any earlier reported *intramolecular* CR processes in synthetic systems,[6−10,15−26] but more importantly, it is comparable to that seen for the bacterial photosynthetic reaction centers.[11]

## Results and Discussion

**Synthesis of the Fc-ZnP-$H_2$P-$C_{60}$ Tetrad.** The preparation of **Fc-ZnP-$H_2$P-$C_{60}$** was carried out as shown in Scheme 1.

(12) (a) Martín, N.; Sánchez, L.; Illescas, B.; Pérez, I. *Chem. Rev.* **1998**, *98*, 2527. (b) Prato, M. *J. Mater. Chem.* **1997**, *7*, 1097. (c) Diederich, F.; Gómez-López, M. *Chem. Soc. Rev.* **1999**, *28*, 263. (d) Sun, Y.-P.; Riggs, J. E.; Guo, Z.; Rollins, H. W. In *Optical and Electronic Properties of Fullerenes and Fullerene-Based Materials*; Shinar, J., Vardeny, Z. V., Kafafi, Z. H., Eds.; Marcel Dekker: New York, 2000; pp 43−81. (e) Guldi, D. M.; Kamat, P. V. In *Fullerenes*; Kadish, K. M., Ruoff, R. S., Eds.; John Wiley & Sons: New York, 2000; Chapter 5, pp 225−281. (f) Fukuzumi, S.; Guldi, D. M. In *Electron Transfer in Chemistry*; Balzani, V., Ed.; Wiley-VCH: Weinheim, 2001; Vol. 2, pp 270−337.

(13) (a) Imahori, H.; Hagiwara, K.; Akiyama, T.; Aoki, M.; Taniguchi, S.; Okada, T.; Shirakawa, M.; Sakata, Y. *Chem. Phys. Lett.* **1996**, *263*, 545. (b) Tkachenko, N. V.; Guenther, C.; Imahori, H.; Tamaki, K.; Sakata, Y.; Fukuzumi, S.; Lemmetyinen, H. *Chem. Phys. Lett.* **2000**, *326*, 344. (c) Imahori, H.; Tamaki, K.; Yamada, H.; Yamada, K.; Sakata, Y.; Nishimura, Y.; Yamazaki, I.; Fujitsuka, M.; Ito, O. *Carbon* **2000**, *38*, 1599. (d) Imahori, H.; Tkachenko, N. V.; Vehmanen, V.; Tamaki, K.; Lemmetyinen, H.; Sakata, Y.; Fukuzumi, S. *J. Phys. Chem. A* **2001**, *105*, 1750. (e) Vehmanen, V.; Tkachenko, N. V.; Imahori, H.; Fukuzumi, S.; Lemmetyinen, H. *Spectrochim. Acta, Part A.* **2001**, *57*, in press.

(14) Guldi, D. M.; Asmus, K.-D. *J. Am. Chem. Soc.* **1997**, *119*, 5744.

(15) (a) Liddell, P. A.; Sumida, J. P.; Macpherson, A. N.; Noss, L.; Seely, G. R.; Clark, K. N.; Moore, A. L.; Moore, T. A.; Gust, D. *Photochem. Photobiol.* **1994**, *60*, 537. (b) Kuciauskas, D.; Lin, S.; Seely, G. R.; Moore, A. L.; Moore, T. A.; Gust, D.; Drovetskaya, T.; Reed, C. A.; Boyd, P. D. W. *J. Phys. Chem.* **1996**, *100*, 15926. (c) Gust, D.; Moore, T. A.; Moore, A. L. *Res. Chem. Intermed.* **1997**, *23*, 621. (d) Liddell, P. A.; Kuciauskas, D.; Sumida, J. P.; Nash, B.; Nguyen, D.; Moore, A. L.; Moore, T. A.; Gust, D. *J. Am. Chem. Soc.* **1997**, *119*, 1400. (e) Carbonera, D.; Di Valentin, M.; Corvaja, C.; Agostini, G.; Giacometti, G.; Liddell, P. A.; Kuciauskas, D.; Moore, A. L.; Moore, T. A.; Gust, D. *J. Am. Chem. Soc.* **1998**, *120*, 4398. (f) Kuciauskas, D.; Liddell, P. A.; Moore, A. L.; Moore, T. A.; Gust, D. *J. Am. Chem. Soc.* **1998**, *120*, 10880. (g) Kuciauskas, D.; Liddell, P. A.; Lin, S.; Johnson, T. E.; Weghorn, S. J.; Lindsey, J. S.; Moore, A. L.; Moore, T. A.; Gust, D. *J. Am. Chem. Soc.* **1999**, *121*, 8604. (h) Kuciauskas, D.; Liddell, P. A.; Lin, S.; Stone, S. G.; Moore, A. L.; Moore, T. A.; Gust, D. *J. Phys. Chem. B* **2000**, *104*, 4307.

(16) (a) Williams, R. M.; Zwier, J. M.; Verhoeven, J. W. *J. Am. Chem. Soc.* **1995**, *117*, 4093. (b) Lawson, J. M.; Oliver, A. M.; Rothenfluh, D. F.; An, Y.-Z.; Ellis, G. A.; Ranasinghe, M. G.; Khan, S. I.; Franz, A. G.; Ganapathi, P. S.; Shephard, M. J.; Paddon-Row, M. N.; Rubin, Y. *J. Org. Chem.* **1996**, *61*, 5032. (c) Williams, R. M.; Koeberg, M.; Lawson, J. M.; An, Y.-Z.; Rubin, Y.; Paddon-Row, M. N.; Verhoeven, J. W. *J. Org. Chem.* **1996**, *61*, 5055. (d) Bell, T. D. M.; Smith, T. A.; Ghiggino, K. P.; Ranasinghe, M. G.; Shephard, M. J.; Paddon-Row, M. N. *Chem. Phys. Lett.* **1997**, *268*, 223.

(17) (a) Jensen, A. W.; Wilson, S. R.; Schuster, D. I. *Bioorg. Med. Chem.* **1996**, *4*, 767. (b) Baran, P. S.; Monaco, R. R.; Khan, A. U.; Schuster, D. I.; Wilson, S. R. *J. Am. Chem. Soc.* **1997**, *119*, 8363. (c) Schuster, D. I.; Cheng, P.; Wilson, S. R.; Prokhorenko, V.; Katterle, M.; Holzwarth, A. R.; Braslavsky, S. E.; Klihm, G.; Williams, R. M.; Luo, C. *J. Am. Chem. Soc.* **1999**, *121*, 11599. (d) Fong, R., II; Schuster, D. I.; Wilson, S. R. *Org. Lett.* **1999**, *1*, 729. (e) Wilson, S. R.; Schuster, D. I.; Nuber, B.; Meier, M. S.; Maggini, M.; Prato, M.; Taylor, R. In *Fullerenes*; Kadish, K. M., Ruoff, R. S., Eds.; John Wiley & Sons: New York, 2000; Chapter 3, pp 91−176.

(18) (a) Nierengarten, J.-F.; Schall, C.; Nicoud, J.-F. *Angew. Chem., Int. Ed.* **1998**, *37*, 1934. (b) Bourgeois, J.-P.; Diederlich, F.; Echegoyen, L.; Nierengarten, J.-F. *Helv. Chim. Acta* **1998**, *81*, 1835. (c) Armaroli, N.; Diederlich, F.; Dietrich-Buchecker, C. O.; Flamigni, L.; Marconi, G.; Nierengarten, J.-F.; Sauvage, J.-P. *Chem. Eur. J.* **1998**, *4*, 406. (d) Armspach, D.; Constable, E. C.; Diederlich, F.; Housecroft, C. E.; Nierengarten, J.-F. *Chem. Eur. J.* **1998**, *4*, 723. (e) Camps, X.; Dietel, E.; Hirsch, A.; Pyo, S.; Echegoyen, L.; Hackbarth, S.; Röder, B. *Chem. Eur. J.* **1999**, *5*, 2362. (f) Armaroli, N.; Marconi, G.; Echegoyen, L.; Bourgeois, J.-P.; Diederlich, F. *Chem. Eur. J.* **2000**, *6*, 1629. (g) van Hal, P. A.; Knol, J.; Langeveld-Voss, B. M. W.; Meskers, S. C. J.; Hummelen, J. C.; Janssen, R. A. J. *J. Phys. Chem. A* **2000**, *104*, 5974. (h) Eckert, J.-F.; Nicoud, J.-F.; Nierengarten, J.-F.; Liu, S.-G.; Echegoyen, L.; Barigelletti, F.; Armaroli, N.; Ouali, L.; Krasnikov, V.; Hadziioannou, G. *J. Am. Chem. Soc.* **2000**, *122*, 7467.

The important synthetic intermediate **3** was prepared by condensation of dipyrromethane **1**[27] with 3,5-di-*tert*-butylbenzaldehyde[28] in the presence of $BF_3OEt_2$, followed by reduction of the nitro group in **2**. Condensation of phenylferrocene acid chloride[29] with diaminoporphyrin **3**, followed by treatment with zinc acetate, gave ferrocene−zincporphyrin **4** in 43% yield. Cross-condensation of porphyrin bis(acid chloride) **5**[22e] with **4** and 4-*tert*-butyldimethylsilyloxymethylaniline[22e] in benzene, followed by deprotection of the *tert*-butyldimethylsilyl group with *n*-$Bu_4NF$, afforded ferrocene−zincporphyrin−freebase-porphyrin **6** in 41% yield. The triad **6** was then converted to the **Fc-ZnP-H$_2$P-C$_{60}$** tetrad using oxidation with $MnO_2$ and subsequent 1,3-dipolar cycloaddition[30] of **7** with $C_{60}$ and *N*-methylglycine in 45% yield (two steps).

**ZnP-H$_2$P-C$_{60}$**,[22e] **Fc-ZnP-C$_{60}$**,[22f] **Fc-H$_2$P-C$_{60}$**,[22f] **ZnP-C$_{60}$**,[22e] **Fc-ref**, and **C$_{60}$-ref**[22f] (Figures 1 and 2) were prepared by following the same procedures as described previously. Structures of all new compounds were confirmed by spectroscopic analysis including $^1$H NMR, IR, and FAB mass spectra. The absorption spectrum of **Fc-ZnP-H$_2$P-C$_{60}$** in PhCN is virtually the superposition of the spectra of the individual chromophores, indicating the lack of strong interaction between the chromophores in the ground state. Similar results were obtained in THF and DMF.

**One-Electron Redox Potentials and ET Driving Force.** An accurate determination of the driving force ($-\Delta G^0_{ET}$) for all the intramolecular ET processes required measuring the redox potentials of **Fc-ZnP-H$_2$P-C$_{60}$** and the reference chromophores (**Fc-ref** and **C$_{60}$-ref**) in various solvents. The differential pulse voltammetry was performed in THF, PhCN, and DMF solutions containing the same supporting electrolyte (i.e., 0.1 M *n*-$Bu_4NPF_6$). Table 1 summarizes all the redox potentials of the investigated compounds. The first one-electron oxidation potential ($E^0_{ox}$) of **Fc-ref** (0.07 V vs ferrocene/ferricenium ($Fc/Fc^+$)) and the first one-electron reduction potential ($E^0_{red}$) of **C$_{60}$-ref** (−1.04 V vs $Fc/Fc^+$) in benzonitrile are the same as those of **Fc-ZnP-H$_2$P-C$_{60}$** in benzonitrile. This further implies that electronic interaction between the ferrocene and the $C_{60}$ is negligible in the ground state. The first one-electron oxidation potential of **Fc-ref** remains nearly constant, despite the substantial increase in solvent polarity.[31] On the other hand, **C$_{60}$-ref** exhibits positive shifts for the underlying first one-electron reduction potentials.[22f,32]

The driving forces ($-\Delta G^0_{ET(CR)}$ in eV) for the intramolecular CR processes from the $C_{60}$ radical anion ($C_{60}^{\bullet-}$) to the freebase porphyrin radical cation ($H_2P^{\bullet+}$), the zincporphyrin radical cation ($ZnP^{\bullet+}$), and the ferricenium ion ($Fc^+$) in **Fc-ZnP-H$_2$P-C$_{60}$** were calculated by eq 1, where *e* stands for the elementary charge.

$$-\Delta G^0_{ET(CR)} = e[E^0_{ox}(D^{\bullet+}/D) - E^0_{red}(A/A^{\bullet-})] \qquad (1)$$

The $-\Delta G^0_{ET(CR)}$ values (in eV), thus obtained in THF, benzonitrile, and DMF, are listed in Table 2. By contrast, the driving force for the intramolecular CS processes ($-\Delta G^0_{ET(CS)}$ in eV) from the freebase porphyrin singlet excited state to the $C_{60}$ was determined by eq 2, where $\Delta E_{0-0}$ is the energy of the

$$-\Delta G^0_{ET(CS)} = \Delta E_{0-0} + \Delta G^0_{ET(CR)} \qquad (2)$$

0−0 transition energy gap between the lowest excited state and the ground state, which is determined by the 0−0* absorption

(19) (a) Thomas, K. G.; Biju, V.; Guldi, D. M.; Kamat, P. V.; George, M. V. *J. Phys. Chem. B* **1999**, *103*, 8864. (b) Thomas, K. G.; Biju, V.; Guldi, D. M.; Kamat, P. V.; George, M. V. *J. Phys. Chem. A* **1999**, *103*, 10755. (c) Tkachenko, N. V.; Rantala, L.; Tauber, A. Y.; Helaja, J.; Hynninen, P. H.; Lemmetyinen, H. *J. Am. Chem. Soc.* **1999**, *121*, 9378. (d) Tkachenko, N. V.; Vuorimaa, E.; Kesti, T.; Alekseev, A. S.; Tauber, A. Y.; Hynninen, P. H.; Lemmetyinen, H. *J. Phys. Chem. B* **2000**, *104*, 6371. (e) Montforts, F.-P.; Kutzki, O. *Angew. Chem., Int. Ed.* **2000**, *39*, 599. (f) D'Souza, F.; Deviprasad, G. R.; Rahman, M. S.; Choi, J.-p. *Inorg. Chem.* **1999**, *38*, 2157.

(20) (a) Guldi, D. M.; Maggini, M.; Scorrano, G.; Prato, M. *J. Am. Chem. Soc.* **1997**, *119*, 974. (b) Maggini, M.; Guldi, D. M.; Mondini, S.; Scorrano, G.; Paolucci. F.; Ceroni, P.; Roffia, S. *Chem. Eur. J.* **1998**, *4*, 1992. (c) Polese, A.; Mondini, S.; Bianco, A.; Toniolo, C.; Scorrano, G.; Guldi, D. M.; Maggini, M. *J. Am. Chem. Soc.* **1999**, *121*, 3446. (d) Da Ros, T.; Prato, M.; Guldi, D. M.; Alessio, E.; Ruzzi, M.; Pasimeni, L. *Chem. Commun.* **1999**, 635. (e) Guldi, D. M.; Luo, C.; Prato, M.; Dietel, E.; Hirsch, A. *Chem. Commun*. **2000**, 373. (f) Guldi, D. M.; Luo, C.; Da Ros, T.; Prato, M.; Dietel, E.; Hirsch, A. *Chem. Commun*. **2000**, 375. (g) Luo, C.; Guldi, D. M.; Maggini, M.; Menna, E.; Mondini, S.; Kotov, N. A.; Prato, M. *Angew. Chem., Int. Ed.* **2000**, *39*, 3905. (h) Guldi, D. M.; Maggini, M.; Martín, N.; Prato, M. *Carbon* **2000**, 38, 1615. (i) Guldi, D. M.; Maggini, M.; Menna, E.; Scorrano, G.; Ceroni, P.; Marcaccio, M.; Paolucci, F.; Roffia, S. *Chem. Eur. J.* **2001**, *7*, 1597. (j) Da Ros, T.; Prato, M.; Guldi, D. M.; Ruzzi, M.; Pasimeni, L. *Chem. Eur. J.* **2001**, *7*, 816. (k) Guldi, D. M.; Luo, C.; Swartz, A.; Scheloske, M.; Hirsch, A. *Chem. Commun.*, **2001**, in press.

(21) (a) Imahori, H.; Hagiwara, K.; Akiyama, T.; Taniguchi, S.; Okada, T.; Sakata, Y. *Chem. Lett.* **1995**, 265. (b) Imahori, H.; Sakata, Y. *Chem. Lett.* **1996**, 199. (c) Imahori, H.; Hagiwara, K.; Aoki, M.; Akiyama, T.; Taniguchi, S.; Okada, T.; Shirakawa, M.; Sakata, Y. *J. Am. Chem. Soc.* **1996**, *118*, 11771. (d) Sakata, Y.; Imahori, H.; Tsue, H.; Higashida, S.; Akiyama, T.; Yoshizawa, E.; Aoki, M.; Yamada, K.; Hagiwara, K.; Taniguchi, S.; Okada, T. *Pure Appl. Chem.* **1997**, *69*, 1951. (e) Tamaki, K.; Imahori, H.; Nishimura, Y.; Yamazaki, I.; Shimomura, A.; Okada, T.; Sakata, Y. *Chem. Lett*. **1999**, 227. (f) Yamada, K.; Imahori, H.; Nishimura, Y.; Yamazaki, I.; Sakata, Y. *Chem. Lett.* **1999**, 895. (g) Imahori, H.; El-Khouly, M. E.; Fujitsuka, M.; Ito, O.; Sakata, Y.; Fukuzumi, S. *J. Phys. Chem. A* **2001**, *105*, 325.

(22) (a) Imahori, H.; Yamada, K.; Hasegawa, M.; Taniguchi, S.; Okada, T.; Sakata, Y. *Angew. Chem., Int. Ed.* **1997**, *36*, 2626. (b) Higashida, S.; Imahori, H.; Kaneda, T.; Sakata, Y. *Chem. Lett.* **1998**, 605. (c) Tamaki, K.; Imahori, H.; Nishimura, Y.; Yamazaki, I.; Sakata, Y. *Chem. Commun.* **1999**, 625. (d) Fujitsuka, M.; Ito, O.; Imahori, H.; Yamada, K.; Yamada, H.; Sakata, Y. *Chem. Lett.* **1999**, 721. (e) Luo, C.; Guldi, D. M.; Imahori, H.; Tamaki, K.; Sakata, Y. *J. Am. Chem. Soc.* **2000**, *122*, 6535. (f) Imahori, H.; Tamaki, K.; Guldi, D. M.; Luo, C.; Fujitsuka, M.; Ito, O.; Sakata, Y.; Fukuzumi, S. *J. Am. Chem. Soc.* **2001**, *123*, 2607. (g) Fukuzumi, S.; Imahori, H.; Yamada, H.; El-Khouly, M. E.; Fujitsuka, M.; Ito, O.; Guldi, D. M. *J. Am. Chem. Soc.* **2001**, *123*, 2571.

(23) (a) Akiyama, T.; Imahori, H.; Ajavakom, A.; Sakata, Y. *Chem. Lett.* **1996**, 907. (b) Imahori, H.; Ozawa, S.; Ushida, K.; Takahashi, M.; Azuma, T.; Ajavakom, A.; Akiyama, T.; Hasegawa, M.; Taniguchi, S.; Okada, T.; Sakata, Y. *Bull. Chem. Soc. Jpn*. **1999**, *72*, 485. (c) Imahori, H.; Yamada, H.; Ozawa, S.; Ushida, K.; Sakata, Y. *Chem. Commun.* **1999**, 1165. (d) Imahori, H.; Yamada, H.; Nishimura, Y.; Yamazaki, I.; Sakata, Y. *J. Phys. Chem. B* **2000**, *104*, 2099. (e) Hirayama, D.; Yamashiro, T.; Takimiya, K.; Aso, Y.; Otsubo, T.; Norieda, H.; Imahori, H.; Sakata, Y. *Chem. Lett.* **2000**, 570. (f) Imahori, H.; Norieda, H.; Yamada, H.; Nishimura, Y.; Yamazaki, I.; Sakata, Y.; Fukuzumi, S. *J. Am. Chem. Soc.* **2001**, *123*, 100. (g) Fukuzumi, S.; Imahori, H. In *Electron Transfer in Chemistry*; Balzani, V., Ed.; Wiley-VCH: Weinheim, 2001; Vol. 2, pp 927−975.

(24) (a) Gust, D.; Moore, T. A.; Moore, A. L.; Lee, S.-J.; Bittersmann, E.; Luttrull, D. K.; Rehms, A. A.; DeGraziano, J. M.; Ma, X. C.; Gao, F.; Belford, R. E.; Trier, T. T. *Science* **1990**, *248*, 199. (b) Gust, D.; Moore, T. A.; Moore, A. L.; Macpherson, A. N.; Lopez, A.; DeGraziano, J. M.; Gouni, I.; Bittersmann, E.; Seely, G. R.; Gao, F.; Nieman, R. A.; Ma, X. C.; Demanche, L. J.; Hung, S.-C.; Luttrull, D. K.; Lee, S.-J.; Kerrigan, P. K. *J. Am. Chem. Soc.* **1993**, *115*, 11141.

(25) (a) Wasielewski, M. R.; Gains, G. L., III; Wiederrecht, G. P.; Svec, W. A.; Niemczyk, M. P. *J. Am. Chem. Soc.* **1993**, *115*, 10442. (b) Wasielewski, M. R.; Wiederrecht, G. P.; Svec, W. A.; Niemczyk, M. P. *Sol. Energy Mater. Solar Cells* **1995**, *38*, 127.

(26) (a) Lendzian, F.; Schlüpmann, J.; von Gersdorff, J.; Möbius, K.; Kurreck, H. *Angew. Chem., Int. Ed. Engl.* **1991**, *30*, 1461. (b) Hasharoni, K.; Levanon, H.; von Gersdorff, J.; Kurreck, H.; Möbius, D. *J. Chem. Phys.* **1993**, *98*, 2916.

(27) Brückner, C.; Karunaratne, V.; Rettig, S. J.; Dolphin, D. *Can. J. Chem.* **1996**, *74*, 2182.

(28) Newman, M. S.; Lee, L. F. *J. Org. Chem.* **1972**, *37*, 4468.

(29) Little, W. F.; Reilley, C. N.; Johnson, J. D.; Lynn, K. N.; Sanders, A. P. *J. Am. Chem. Soc.* **1964**, *86*, 1376.

(30) Maggini, M.; Scorrano, G.; Prato, M. *J. Am. Chem. Soc.* **1993**, *115*, 9798.

(31) Gagné, R. R.; Koval, C. A.; Lisensky, G. C. *Inorg. Chem.* **1980**, *19*, 2855.

(32) Dubois, D.; Moninot, G.; Kutner, W.; Jones, M. T.; Kadish, K. M. *J. Phys. Chem.* **1992**, *96*, 7137.

**Scheme 1**

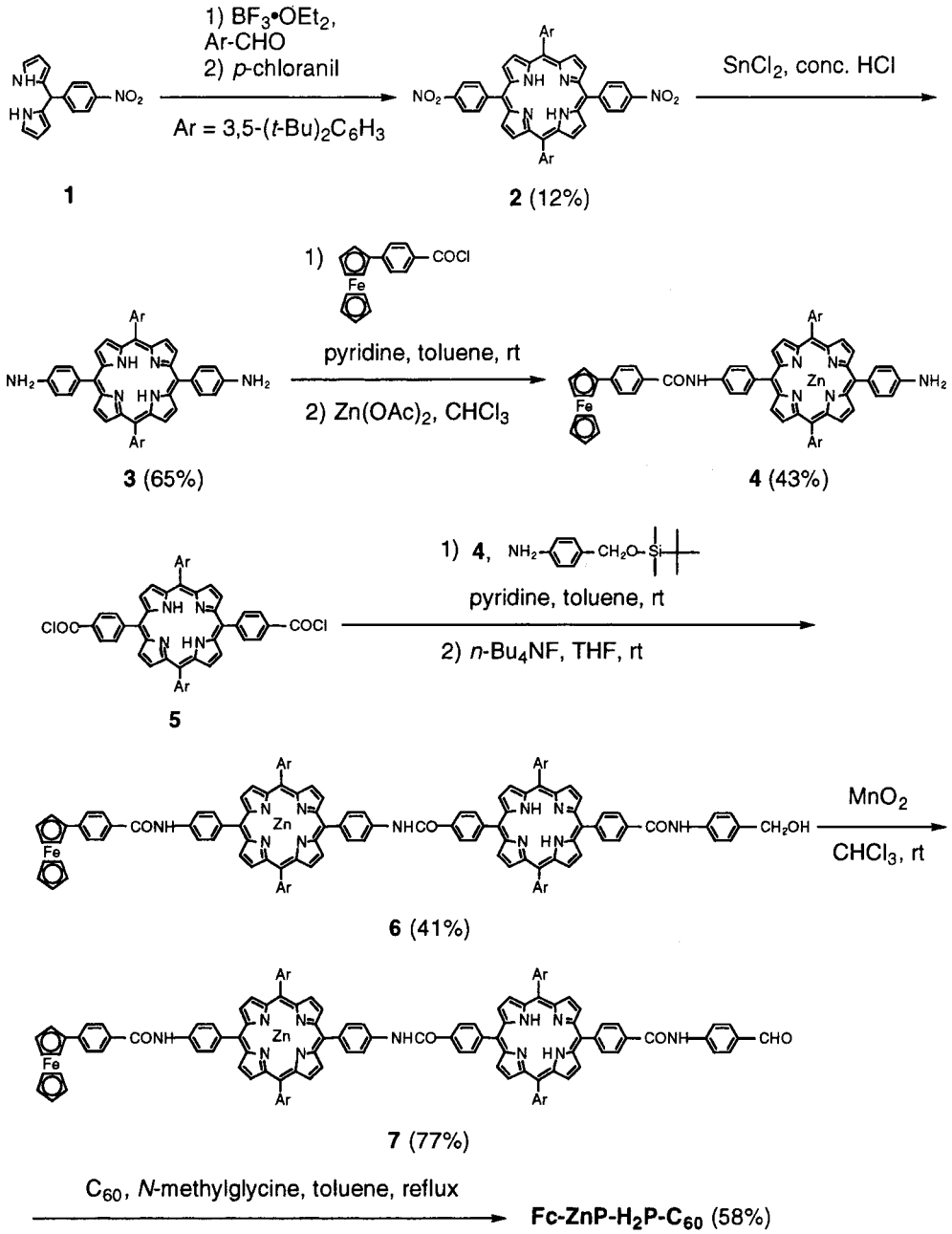


and $0^{*}-0$ fluorescence maxima in condensed media (the asterisk denotes the excited state). The $-\Delta G^{0}_{ET(CS)}$ values are given in Table 2. The driving forces for intramolecular charge-shift (CSH) processes ($-\Delta G^{0}_{ET(CSH)}$ in eV) from the ZnP to the $H_2P^{\bullet+}$ and from the Fc to the $ZnP^{\bullet+}$ in **Fc-ZnP-H$_2$P-C$_{60}$** were determined by subtracting the energy of the final state from that of the initial state (Table 2). It should be noted that the Coulombic terms in the present donor−acceptor systems are negligible, especially in solvents with moderate or high polarity, because of the relatively long edge-to-edge distance ($R_{ee}$ > 11 Å) employed.

**Photodynamics of Fc-ZnP-H$_2$P-C$_{60}$.** Successful mimicry of primary events in photosynthesis using **ZnP-H$_2$P-C$_{60}$**[22e] and **Fc-ZnP-C$_{60}$**[22d,f] encouraged us to combine these two systems into an integrated single system (**Fc-ZnP-H$_2$P-C$_{60}$**). Since a ferrocene unit is tethered at the end of **ZnP-H$_2$P-C$_{60}$**, the tetrad will display coupled photoinduced EN and ET, namely, **Fc-$^{1}$ZnP$^{*}$-H$_2$P-C$_{60}$** (2.04 eV) → **Fc-ZnP-$^{1}$H$_2$P$^{*}$-C$_{60}$** (1.89 eV) → **Fc-ZnP-H$_2$P$^{\bullet+}$-C$_{60}^{\bullet-}$** (1.63 eV) → **Fc-ZnP$^{\bullet+}$-H$_2$P-C$_{60}^{\bullet-}$** (1.34 eV) → **Fc$^{+}$-ZnP-H$_2$P-C$_{60}^{\bullet-}$** (1.11 eV) in polar media (Scheme 2). The final charge separated state ($Fc^{+}$ and $C_{60}^{\bullet-}$ pair) is characterized by a large $R_{ee}$ value of 48.9 Å. Time-resolved transient absorption spectra, following picosecond and nanosecond laser pulses, were employed to examine the photodynamics of **Fc-ZnP-H$_2$P-C$_{60}$** (vide infra).

At first, the photodynamics of the triad systems (**ZnP-H$_2$P-C$_{60}$** and **Fc-ZnP-C$_{60}$**) are described for the better understanding of the more complex tetrad system. We reported the photophysics of **ZnP-H$_2$P-C$_{60}$** in benzonitrile in detail (Scheme 3).[22e] An initial singlet−singlet EN from $^{1}ZnP^{*}$ (2.04 eV) to $H_2P$ (1.89 eV) ($k_{EN} = 1.5 \times 10^{10}$ s$^{-1}$) is followed by a sequential ET relay evolving from the **ZnP-$^{1}$H$_2$P*-C$_{60}$** (CS1) to yield **ZnP-H$_2$P$^{\bullet+}$-C$_{60}^{\bullet-}$** (1.63 eV) and subsequently **ZnP$^{\bullet+}$-H$_2$P-C$_{60}^{\bullet-}$** (1.34 eV) via CSH1. Thereby, the individual rate constants $k_{ET(CS1)}$ and $k_{ET(CSH1)}$ were determined as $7.0 \times 10^{9}$ and $2.2 \times 10^{9}$ s$^{-1}$, respectively.[22e] The final charge-separated state, formed in moderate quantum yields (0.40), decays directly to the ground state with a rate constant ($k_{ET(CR2)}$) of $4.8 \times 10^{4}$ s$^{-1}$ as analyzed from the decay kinetics of the $C_{60}^{\bullet-}$ absorption (ca. 1000

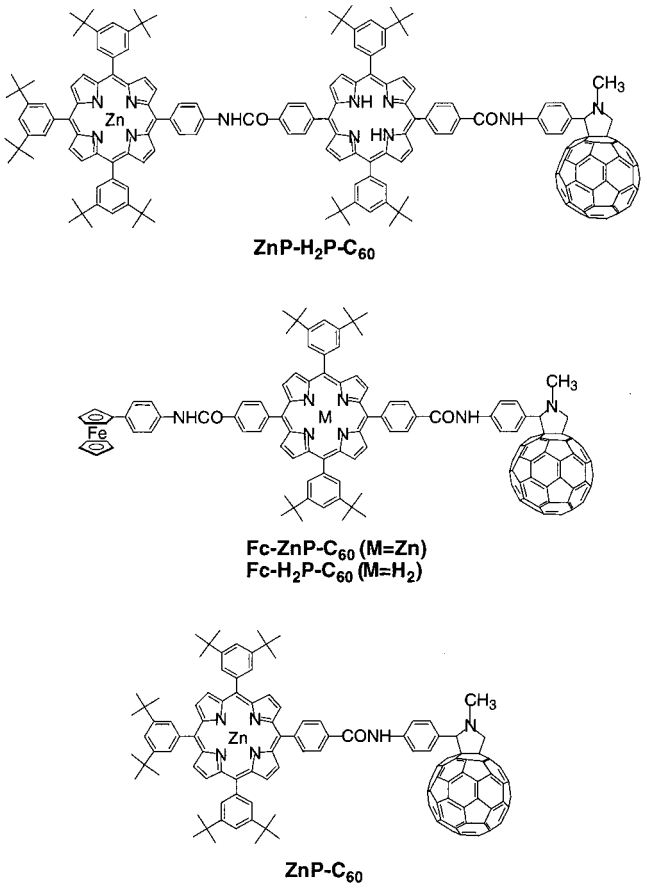


**Figure 2.** Structures of porphyrin−fullerene linked triads and dyad.

**Table 1.** One-Electron Redox Potentials (vs $Fc/Fc^+$)[a] of Tetrad and the References in Various Solvents

| | | $E^0_{ox}$/V | | $E^0_{red}$/V | |
|---|---|---|---|---|---|
| compound | solvent | $H_2P^{\bullet+}/H_2P$ | $ZnP^{\bullet+}/ZnP$ | $Fc^+/Fc$ | $C_{60}/C_{60}^{\bullet-}$ |
| **Fc-ZnP-H$_2$P-C$_{60}$** | benzonitrile | 0.59 | 0.30 | 0.07 | −1.04 |
| **Fc-ref**, **C$_{60}$-ref** | THF | | | 0.05 | −1.02[b] |
| **Fc-ref**, **C$_{60}$-ref** | benzonitrile | | | 0.07 | −1.04[b] |
| **Fc-ref**, **C$_{60}$-ref** | DMF | | | 0.06 | −0.92[b] |

[a] The redox potentials were measured by differential pulse voltammetry in THF, benzonitrile, and DMF using 0.1 M *n*-$Bu_4NPF_6$ as a supporting electrolyte with a sweep rate of 10 mV $s^{-1}$. [b] From ref 22f.

nm[22e,33]). By analyzing the decay kinetics of the $C_{60}^{\bullet-}$ fingerprint at 1000 nm, the ET rate constants for CR in **ZnP**$^{\bullet+}$**-H$_2$P-C$_{60}$**$^{\bullet-}$ ($k_{ET(CR2)}$) were also determined as $2.9 \times 10^4$ (THF) and $5.0 \times 10^4$ $s^{-1}$ (DMF) (Table 3).[22f] The total quantum yields of CS in **ZnP-H$_2$P-C$_{60}$** ($\Phi_{CS}$(total)) were estimated from the transient absorption spectra as 0.26 in THF and 0.21 in DMF, respectively.[22f] The relatively low quantum yields (0.21−0.40) can be explained by the competition of the CSH from **ZnP-H$_2$P**$^{\bullet+}$**-C$_{60}$**$^{\bullet-}$ (1.63 eV) to **ZnP**$^{\bullet+}$**-H$_2$P-C$_{60}$**$^{\bullet-}$ (1.34 eV) versus the decay of **ZnP-H$_2$P**$^{\bullet+}$**-C$_{60}$**$^{\bullet-}$ to the triplet excited states of the freebase porphyrin ($^3H_2P^*$ (1.40 eV)) and the $C_{60}$ ($^3C_{60}^*$ (1.50 eV)).[22f] The decay of **ZnP-H$_2$P**$^{\bullet+}$**-C$_{60}$**$^{\bullet-}$ to the ground state is negligible because of the slow CR1 rate ($\sim 10^4$ $s^{-1}$) estimated from the Marcus parabola for **ZnP-C$_{60}$** (vide infra).

We also reported the photodynamics of **Fc-ZnP-C$_{60}$** in various solvents.[22d,f] Based on the energy level of each state in benzonitrile, initial photoinduced CS occurs from all the excited states (i.e., the porphyrin singlet excited state ($^1ZnP^*$ (2.04 eV)), the porphyrin triplet excited state ($^3ZnP^*$ (1.53 eV)), the $C_{60}$ singlet excited state ($^1C_{60}^*$ (1.75 eV)), and the $C_{60}$ triplet excited state ($^3C_{60}^*$ (1.50 eV))) to the counterpart within the molecule to produce **Fc-ZnP**$^{\bullet+}$**-C$_{60}$**$^{\bullet-}$ (1.21−1.42 eV).[22f] The photodynamical behavior is similar to that of **ZnP**−**C$_{60}$**.[21g] The CS rates from $^1ZnP^*$, $^1C_{60}^*$, and $^3C_{60}^*$ in **ZnP-C$_{60}$**, together with the CR rates of **ZnP**$^{\bullet+}$**-C$_{60}$**$^{\bullet-}$ in various solvents, were reported previously[21g,22f] and are summarized in Table 3. The resulting transient **Fc-ZnP**$^{\bullet+}$**-C$_{60}$**$^{\bullet-}$ state undergoes a subsequent and rapid CSH to generate the final **Fc**$^+$**-ZnP-C$_{60}$**$^{\bullet-}$ state with a rate constant of $2.8 \times 10^9$ $s^{-1}$ in benzonitrile.[22f] The efficiency of CSH from the Fc to the $ZnP^{\bullet+}$ in **Fc-ZnP**$^{\bullet+}$**-C$_{60}$**$^{\bullet-}$ was found to be nearly unity.[22f] A similar photodynamical behavior was noted in THF and DMF solutions.[22d,f] By analyzing the decay kinetics of the $C_{60}^{\bullet-}$ fingerprint at 1000 nm,[22e,33] the ET rate constants for CR in **Fc**$^+$**-ZnP-C$_{60}$**$^{\bullet-}$ were determined as $2.7 \times 10^5$ (THF), $1.3 \times 10^5$ (benzonitrile), and $6.3 \times 10^4$ $s^{-1}$ (DMF) (Table 3).[22d,f] The total quantum yields of CS ($\Phi_{CS}$(total)) in **Fc-ZnP-C$_{60}$** were found to be 0.74 in THF, 0.85 in PhCN, and 0.36 in DMF by the comparative method[22e] from the corresponding transient absorption spectra.[22f] **Fc-H$_2$P-C$_{60}$** exhibits similar photodynamical behavior in THF, benzonitrile, and DMF.[22f] The CS and CR rates and the corresponding driving forces in **Fc-ZnP-C$_{60}$** and **Fc-H$_2$P-C$_{60}$** were reported previously[22d,f] and are summarized in Table 3.

Taking into account the similarity in molecular structures of **Fc-ZnP-H$_2$P-C$_{60}$** (Figure 1), **ZnP-H$_2$P-C$_{60}$**, and **Fc-ZnP-C$_{60}$** (Figure 2), we can expect similar photodynamics in **Fc-ZnP-H$_2$P-C$_{60}$** (Scheme 2). Transient absorption spectra, recorded at various time delays following a short 18 ps laser excitation in deoxygenated benzonitrile, shed light onto the cascade of intramolecular reactions in photoexcited **Fc-ZnP-H$_2$P-C$_{60}$** (Figure 3). The absorption ratio (ZnP:$H_2P$ = 1:2) of the two porphyrin chromophores (i.e., ZnP and $H_2P$) at the 532 nm laser excitation leads unavoidably to the population of the singlet excited state of both porphyrin moieties, ZnP (2.04 eV) and $H_2P$ (1.89 eV). Considering the energy gap between the two singlet excited states (0.15 eV) with the lower state being that of $H_2P$, a rapid singlet−singlet EN prevails with a time constant of $k_{EN} = 2.6 \times 10^{10}$ $s^{-1}$. Importantly, the measured EN rate closely resembles the dynamics of **ZnP-H$_2$P-C$_{60}$** (vide supra) and the time-resolved fluorescence measurements ($2.2 \times 10^{10}$ $s^{-1}$).[22c] Kinetic evidence for this transfer stems from the grow-in of the singlet excited-state absorption features of $H_2P$ around 650−760 nm,[22e] which took place in two distinguishable steps (Figure 3a,b). The faster process, which is masked by the apparatus' time resolution (<20 ps), refers to the direct route, which is the excitation of $H_2P$. By contrast, the slower, indirect route results from the actual EN event between the two porphyrin moieties. The 760 nm kinetic trace (Figure 3b) illustrates the grow-in of the $H_2P$ singlet−singlet absorption. In the wavelength region between 500 and 530 nm, the singlet−singlet absorption of the $H_2P$ chromophore is, however, weaker than that of the ZnP precursor. Here the actual energy transfer event is associated with a loss of absorption, as shown in the 525 nm kinetic trace of Figure 3b.

The conclusion of the initial singlet excited-state energy migration is a high-lying and very reactive $^1H_2P^*$ (1.89 eV), which is located adjacent to the electron and energy accepting fullerene. $^1H_2P^*$ is the starting point for the formation of **Fc-ZnP-H$_2$P**$^{\bullet+}$**-C$_{60}$**$^{\bullet-}$ (1.63 eV) via CS1, as in the case of **ZnP-H$_2$P-C$_{60}$**. CS from **Fc-ZnP-H$_2$P-**$^1$**C$_{60}$*** could not be confirmed by fluorescence lifetime measurements, because of the extensive

(33) Guldi, D. M.; Hungerbühler, H.; Asmus, K.-D. *J. Phys. Chem.* **1995**, *99*, 9380.

**Table 2.** Rate Constants ($k_{ET}$ and $k_{EN}$) and the Driving Forces ($-\Delta G^0_{ET}$ and $-\Delta G^0_{EN}$) of **Fc-ZnP-H$_2$P-C$_{60}$** in Solutions

| solvent | initial state[a] | final state[a] | $-\Delta G^0$/eV | $k$/s$^{-1}$[b] | $\Phi_{CS}$(total)[c] |
|---|---|---|---|---|---|
| THF ($\epsilon_s = 7.58$) | Fc$^+$-ZnP-H$_2$P-C$_{60}^{\bullet-}$ (1.07 eV) | Fc-ZnP-H$_2$P-C$_{60}$ | 1.07 | $k_{ET(CR3)} < 10^2$ | 0.20 |
| benzonitrile ($\epsilon_s = 25.2$) | Fc-$^1$ZnP*-H$_2$P-C$_{60}$ (2.04 eV) | Fc-ZnP-$^1$H$_2$P*-C$_{60}$ (1.89 eV) | 0.15 | $k_{EN} = 2.6 \times 10^{10}$ | |
| | Fc-ZnP-$^1$H$_2$P*-C$_{60}$ (1.89 eV) | Fc-ZnP-H$_2$P$^{\bullet+}$-C$_{60}^{\bullet-}$ (1.63 eV) | 0.26 | $k_{ET(CS1)} = 6.9 \times 10^9$ | |
| | Fc-ZnP-H$_2$P$^{\bullet+}$-C$_{60}^{\bullet-}$ (1.63 eV) | Fc-ZnP$^{\bullet+}$-H$_2$P-C$_{60}^{\bullet-}$ (1.34 eV) | 0.29 | $k_{ET(CSH1)} = 2.5 \times 10^9$ | |
| | Fc-ZnP$^{\bullet+}$-H$_2$P-C$_{60}^{\bullet-}$ (1.34 eV) | Fc$^+$-ZnP-H$_2$P-C$_{60}^{\bullet-}$ (1.11 eV) | 0.23 | $k_{ET(CSH2)} = 1.7 \times 10^8$ | |
| | Fc$^+$-ZnP-H$_2$P-C$_{60}^{\bullet-}$ (1.11 eV) | Fc-ZnP-H$_2$P-C$_{60}$ | 1.11 | $k_{ET(CR3)} < 10^2$ | 0.24 |
| DMF ($\epsilon_s = 36.7$) | Fc$^+$-ZnP-H$_2$P-C$_{60}^{\bullet-}$ (0.98 eV) | Fc-ZnP-H$_2$P-C$_{60}$ | 0.98 | $k_{ET(CR3)} < 10^2$ | 0.17 |

[a] The energy of each state relative to the ground state is given in parentheses. [b] The $k_{ET}$ values for CS, CR, and CSH and the $k_{EN}$ value were determined by transient absorption spectroscopy. [c] The total quantum yield of CS based on the comparative method.[22e]

**Scheme 2.** Reaction Scheme and Energy Diagram for **Fc-ZnP-H$_2$P-C$_{60}$** in Benzonitrile

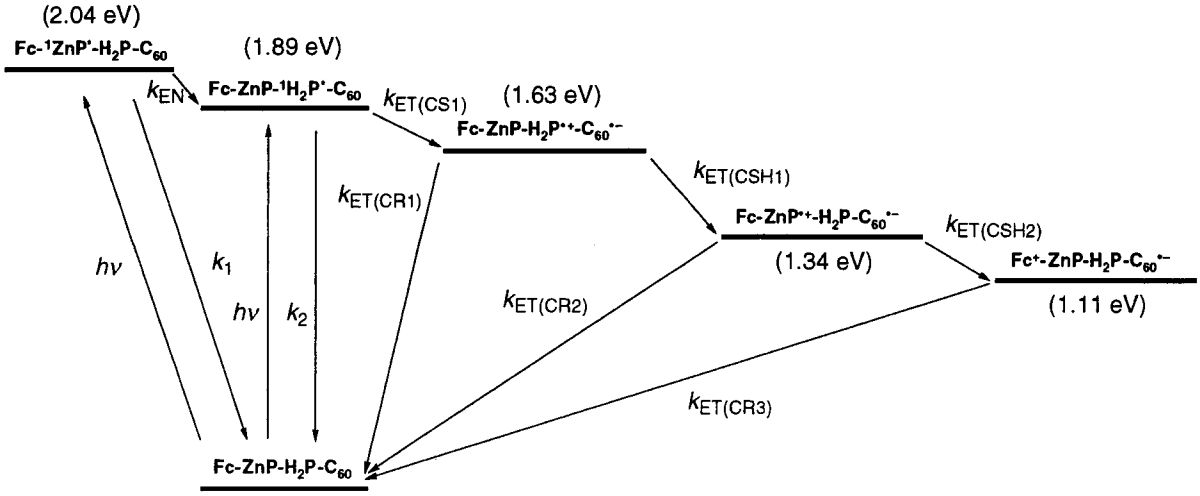


**Scheme 3.** Reaction Scheme and Energy Diagram for **ZnP-H$_2$P-C$_{60}$** in Benzonitrile

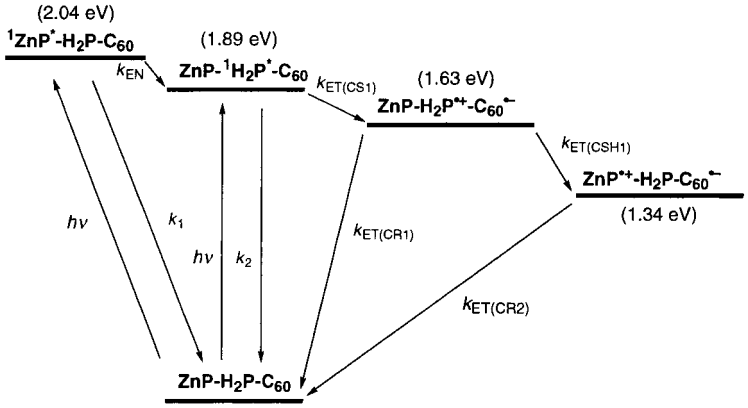


overlap between the free base porphyrin emission ($\lambda_{max} = 655$, 720 nm) and the C$_{60}$ emission ($\lambda_{max} = 720$ nm). However, the fullerene singlet excited state (1.75 eV) may also undergo CS from the H$_2$P to generate **Fc-ZnP-H$_2$P$^{\bullet+}$-C$_{60}^{\bullet-}$**, which is a minor process judging from the relative ratio of the C$_{60}$ absorption (<10%) at 532 nm.[21g,22e,f] Spectroscopically, the oxidized donor, H$_2$P$^{\bullet+}$, was identified by a strong absorption in the visible (i.e., 600−800 nm, see Figure 4a).[22e,34] Hereby, the formation kinetics of the $\pi$-radical cation in the visible and the fullerene $\pi$-radical anion in the near-infrared (i.e., 1000 nm)[22e,33] are valuable aids in determining the absolute rate constants, providing similar values ($k_{ET(CS1)}$) of $7.1 \times 10^9$ and $6.7 \times 10^9$ s$^{-1}$, respectively. Exemplifying time−absorption profiles in the visible are given in Figure 3b, showing the first CS step at 525 and 760 nm. Precisely at 760 nm CS is associated with a monoexponential decay of the $^1$H$_2$P* absorption to the weaker absorbing **Fc-ZnP-H$_2$P$^{\bullet+}$-C$_{60}^{\bullet-}$**, while at 525 nm a biexponential rate law was found to govern the kinetics in the time window up to 250 ps. Here, the biexponential decay is constituted by the fast EN ($k_{EN} = 2.6 \times 10^{10}$ s$^{-1}$) and slower CS ($k_{ET(CS1)} = 7.1 \times 10^9$ s$^{-1}$).

The absorption of the H$_2$P $\pi$-radical cation, as it emerged from the CS process, is subject to a rapid intramolecular decay.

(34) Gasyna, Z.; Browett, W. R.; Stillman, M. J. *Inorg. Chem.* **1985**, *24*, 2440.

**Table 3.** Free Energy Changes ($-\Delta G^0_{ET}$) and ET Rate Constants ($k_{ET}$) for CS and CR in Fullerene-Based Dyad, Triads, and Tetrad at 298 K

| | THF ($\epsilon_s = 7.58$) | | benzonitrile ($\epsilon_s = 25.2$) | | DMF ($\epsilon_s = 36.7$) | |
|---|---|---|---|---|---|---|
| initial state | $-\Delta G^0_{ET}$/eV | $k_{ET}/s^{-1}$ | $-\Delta G^0_{ET}$/eV | $k_{ET}/s^{-1}$ | $-\Delta G^0_{ET}$/eV | $k_{ET}/s^{-1}$ |
| **$^1$ZnP*-C$_{60}$** | 0.65[a] | $1.3 \times 10^{10}$ [b] | 0.66[a] | $9.5 \times 10^{9}$ [c] | 0.85[a] | $1.3 \times 10^{10}$ [b] |
| **ZnP-$^1$C$_{60}$*** | 0.33[a] | $5.1 \times 10^{8}$ [a] | 0.37[a] | $5.5 \times 10^{8}$ [c] | *d* | *d* |
| **ZnP-$^3$C$_{60}$*** | 0.08[a] | $1.6 \times 10^{7}$ [a] | 0.12[a] | $1.5 \times 10^{7}$ [c] | *d* | *d* |
| **ZnP$^{\bullet+}$-C$_{60}^{\bullet-}$** | 1.42[a] | $3.7 \times 10^{5}$ [a] | 1.38[a] | $1.3 \times 10^{6}$ [c] | 1.21[a] | $1.8 \times 10^{6}$ [a] |
| **Fc$^+$-ZnP-C$_{60}^{\bullet-}$** | 1.00[a] | $2.7 \times 10^{5}$ [e] | 1.03[a] | $1.3 \times 10^{5}$ [e] | 0.91[a] | $6.3 \times 10^{4}$ [e] |
| **Fc$^+$-H$_2$P-C$_{60}^{\bullet-}$** | *d* | *d* | 1.03[a] | $1.2 \times 10^{5}$ [a] | 0.91[a] | $5.3 \times 10^{4}$ [a] |
| **ZnP$^{\bullet+}$-H$_2$P-C$_{60}^{\bullet-}$** | 1.37[a] | $2.9 \times 10^{4}$ [a] | 1.34[a] | $4.8 \times 10^{4}$ [f] | 1.17[a] | $5.0 \times 10^{4}$ [a] |
| **Fc$^+$-ZnP-H$_2$P-C$_{60}^{\bullet-}$** | 1.07 | *d* | 1.11 | 2.9[g] | 0.98 | 3.7[g] |

[a] From ref 22f. [b] From ref 21f. [c] From ref 21g. [d] Not determined. [e] From ref 22d. [f] From ref 22e. [g] Extrapolated using eq 5.

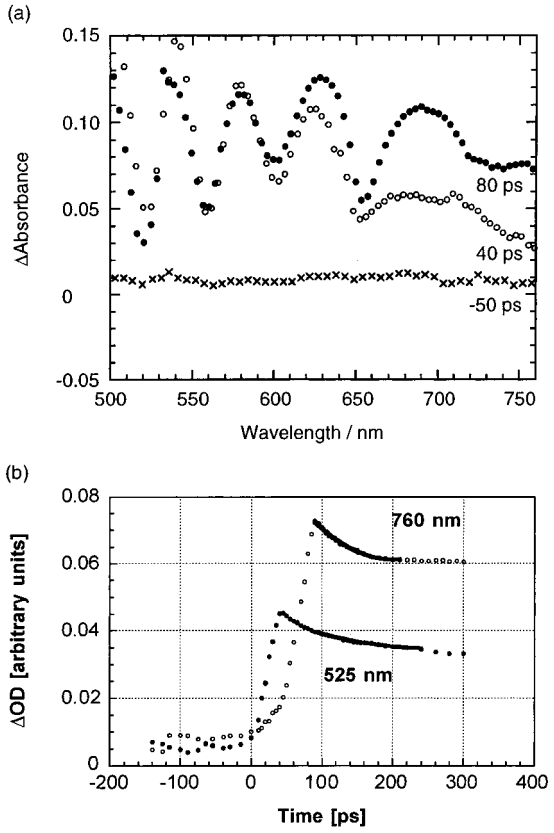


**Figure 3.** Differential absorption spectra obtained upon picosecond flash photolysis (532 nm) of $\sim 10^{-5}$ M solutions of **Fc-ZnP-H$_2$P-C$_{60}$** tetrad in nitrogen-saturated benzonitrile with a time delay of (a) $-50$ (cross), 40 (open circle), and 80 ps (solid circle) and (b) time−absorption profiles at 525 (solid circle) and 760 nm (open circle).

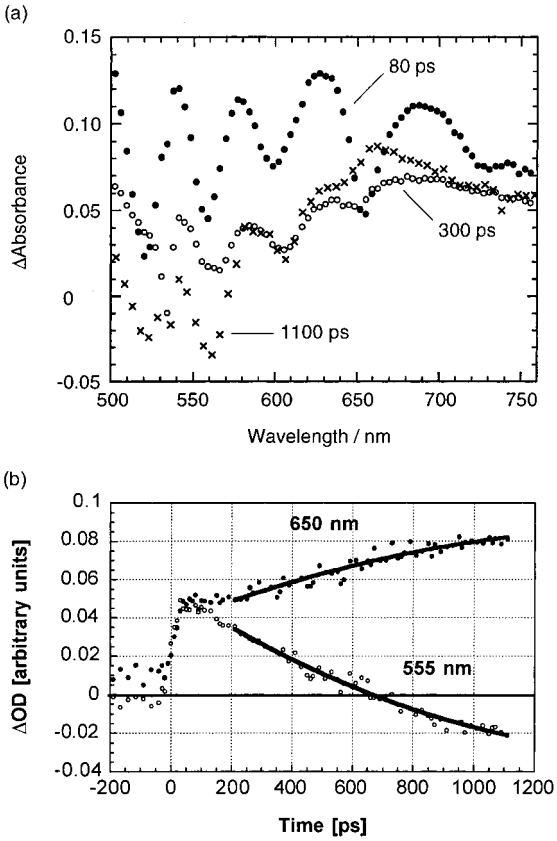


**Figure 4.** Differential absorption spectra obtained upon picosecond flash photolysis (532 nm) of $\sim 10^{-5}$ M solutions of **Fc-ZnP-H$_2$P-C$_{60}$** tetrad in nitrogen saturated benzonitrile with a time delay of (a) 80 (solid circle), 300 (open circle), and 1100 ps (cross) and (b) time−absorption profiles at 555 (open circle) and 650 nm (solid circle).

The product of this deactivation ($k_{ET(CSH1)} = 2.5 \times 10^9$ s$^{-1}$) is a differential absorption spectrum, which displays the ZnP $\pi$-radical cation absorption with a maximum at 650 nm (Figure 4a).[22e,35] Time−absorption profiles (Figure 4b), which unravel both the formation (ZnP$^{\bullet+}$) and also the decay (H$_2$P$^{\bullet+}$) kinetics at 650 and 555 nm, respectively, corroborate that the underlying rates are nearly identical. Furthermore, the new transient (Figure 4a) is identical with that noted for the final charge-separated radical pair (**ZnP$^{\bullet+}$-H$_2$P-C$_{60}^{\bullet-}$**) in the above-described **ZnP-H$_2$P-C$_{60}$** triad.[22e] Taking the spectroscopic and kinetic evidence in concert, we reach the conclusion that the resulting species evolves from a first CSH between the two porphyrin donors yielding the **Fc-ZnP$^{\bullet+}$-H$_2$P-C$_{60}^{\bullet-}$** radical pair (1.34 eV). It is imperative to note that this energy level (1.34 eV) falls substantially below that of any singlet or triplet excited states of ZnP, H$_2$P, and C$_{60}$, thereby ruling out the subsequent formation of an excited state as a product of CR. In fact, the long-lived **ZnP$^{\bullet+}$-H$_2$P-C$_{60}^{\bullet-}$** ($k_{ET(CR2)} = 4.8 \times 10^4$ s$^{-1}$), which can be taken as a suitable model, is known to regenerate the singlet ground state quantitatively.

In line with the thermodynamics, which predict a second, exothermic (0.23 eV) CSH reaction from the end-terminus Fc to ZnP$^{\bullet+}$, the 650 nm maximum of ZnP$^{\bullet+}$ decreases further (Figure 5a). Importantly, the final photoproduct, **Fc$^+$-ZnP-H$_2$P-C$_{60}^{\bullet-}$**, bears no spectral resemblance to the transient intermediates constituted in part by either of the strongly absorbing ZnP$^{\bullet+}$ or H$_2$P$^{\bullet+}$ $\pi$-radical cations in **Fc-ZnP$^{\bullet+}$-H$_2$P-C$_{60}^{\bullet-}$** and **Fc-ZnP-H$_2$P$^{\bullet+}$-C$_{60}^{\bullet-}$**, respectively. Similarly, the bleaching of the ZnP and H$_2$P Q-band absorption (i.e., 500−600 nm), which is an additional attribute of the one-electron oxidized porphyrins, is completely lacking. The actual rate constant for this second CSH reaction ($k_{ET(CSH2)} = 1.7 \times 10^8$ s$^{-1}$) could be derived with reasonable accuracy from the time−absorption profiles. The

(35) (a) Fuhrhop, J.-H.; Mauzerall, D. *J. Am. Chem. Soc.* **1969**, *91*, 4174. (b) Chosrowjan, H.; Taniguchi, S.; Okada, T.; Takagi, S.; Arai, T.; Tokumaru, K. *Chem. Phys. Lett.* **1995**, *242*, 644.

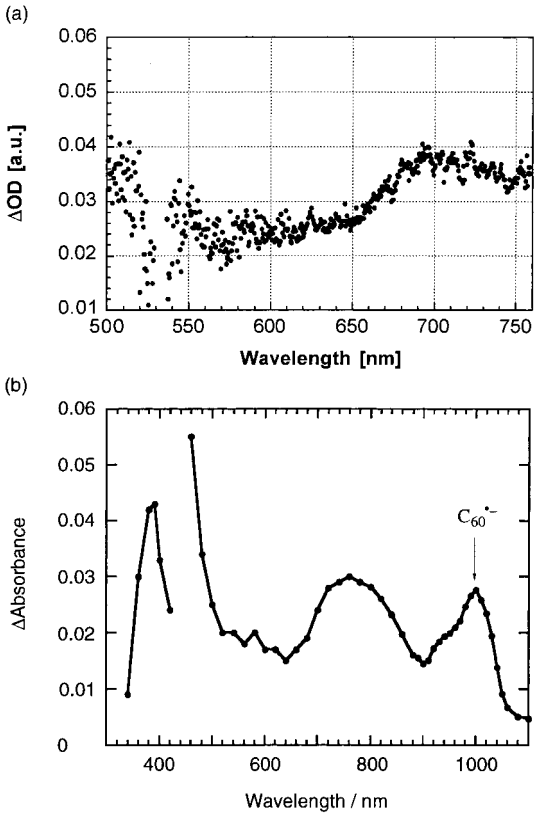


**Figure 5.** (a) Differential absorption spectra obtained upon picosecond flash photolysis (532 nm) of $\sim 10^{-5}$ M solutions of **Fc-ZnP-H$_2$P-C$_{60}$** tetrad in nitrogen-saturated benzonitrile with a time delay of 6 ns and (b) differential absorption spectra obtained upon nanosecond flash photolysis (532 nm) of $7.2 \times 10^{-6}$ M solutions of **Fc-ZnP-H$_2$P-C$_{60}$** tetrad in nitrogen-saturated benzonitrile with a time delay of 50 ns at 298 K.

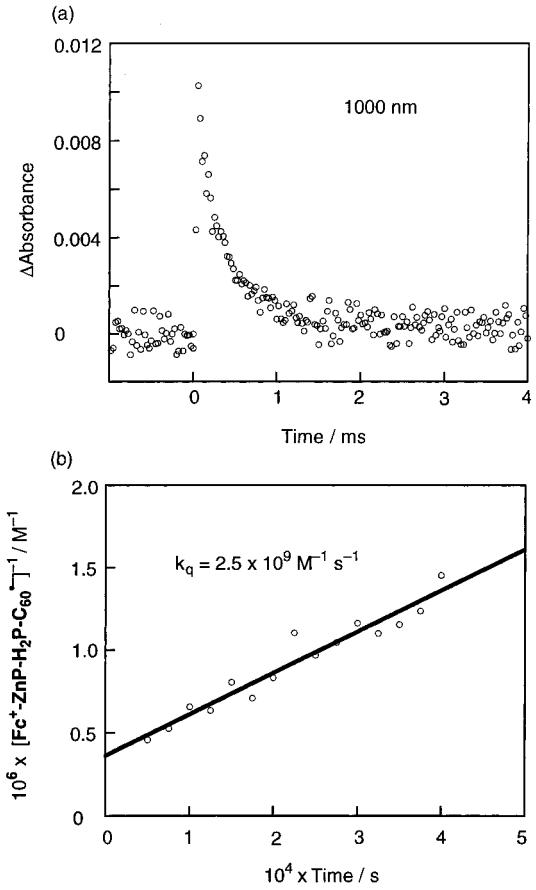


**Figure 6.** (a) The time profile of absorbance at 1000 nm obtained by nanosecond time-resolved absorption spectra of **Fc-ZnP-H$_2$P-C$_{60}$** tetrad ($3.6 \times 10^{-6}$ M) in argon-saturated DMF excited at 532 nm at 298 K. (b) Second-order plot derived from the absorption change at 1000 nm.

CSH2 rate is slower by 1 order of magnitude than the corresponding CSH value ($2.8 \times 10^9\ s^{-1}$) of **Fc-ZnP-C$_{60}$** in PhCN.[22f] The reversal of the amide bond between the ferrocene and the zincporphyrin in **Fc-ZnP-H$_2$P-C$_{60}$** and **Fc-ZnP-C$_{60}$** has its impact on the driving force (0.23 eV (**Fc-ZnP-H$_2$P-C$_{60}$**) versus 0.35 eV (**Fc-ZnP-C$_{60}$**)). Thus, the attenuation of the CSH2 rate in **Fc-ZnP-H$_2$P-C$_{60}$** can be explained by the difference in the driving force. On the other hand, the spectral changes in the near-infrared, due to the fullerene $\pi$-radical anion, remained constant, throughout the cascade of CSH reactions.

Nanosecond transient absorption studies following laser excitation of **Fc-ZnP-H$_2$P-C$_{60}$** reveal unambiguously the $C_{60}^{\bullet-}$ fingerprint (ca. 1000 nm), which matches quite reasonably that known for the $\pi$-radical anion of a *N*-methylfulleropyrrolidine (Figure 5b).[22e,33] In regard to the oxidized donor part, the weak absorption features of the ferricenium ion ($Fc^+$: $\lambda_{max} \sim$ 800 nm ($\epsilon \sim 1000\ M^{-1}\ cm^{-1}$))[36] have prevented its direct detection. As such, the UV−visible changes are dominated by the differential absorption changes, which are associated with the one-electron reduction of the fullerene, especially around 400 nm. Since no absorption bands due to the $ZnP^{\bullet+}$ [35] or $H_2P^{\bullet+}$ [34] were detected together with the absorption due to the reduced part ($C_{60}^{\bullet-}$), the oxidized part must be $Fc^+$ (Scheme 2). In fact, the transient absorption spectra of **Fc-ZnP-H$_2$P-C$_{60}$** (Figure 5) are virtually the same as those of **Fc$^+$-ZnP-C$_{60}^{\bullet-}$** and **Fc$^+$-H$_2$P-C$_{60}^{\bullet-}$**.[22f,g] **Fc-ZnP-H$_2$P-C$_{60}$** exhibits similar photodynamical behavior in THF and DMF. On the basis of the predominant excitation of the ZnP moiety, the total quantum yields ($\Phi_{CS}$(total)) for CS of 0.20 (THF), 0.24 (PhCN), and 0.17 (DMF) were determined (Table 2), by applying the comparative method from the nanosecond time-resolved transient spectra [monofunctionalized $C_{60}^{\bullet-}$ ($\epsilon_{1000\ nm} = 4700\ M^{-1}\ cm^{-1}$)].[22e] The relatively low quantum yields (0.17−0.24) can be rationalized by the competition of the CSH from **Fc-ZnP-H$_2$P$^{\bullet+}$-C$_{60}^{\bullet-}$** (1.63 eV) to **Fc-ZnP$^{\bullet+}$-H$_2$P-C$_{60}^{\bullet-}$** (1.34 eV) versus the decay of **Fc-ZnP-H$_2$P$^{\bullet+}$-C$_{60}^{\bullet-}$** to the triplet states of the freebase porphyrin (1.40 eV) and the $C_{60}$ (1.50 eV), which is similar to that of **ZnP-H$_2$P-C$_{60}$** (vide supra).

In contrast to the primary building blocks of the present tetrad (**ZnP-C$_{60}$**, **Fc-ZnP-C$_{60}$**, and **ZnP-H$_2$P-C$_{60}$**), the decay dynamics of the charge-separated radical pair (**Fc$^+$-ZnP-H$_2$P-C$_{60}^{\bullet-}$**) does not obey first-order kinetics. The time profiles at 1000 nm (i.e., at the maximum of the $C_{60}^{\bullet-}$ absorption) obey instead second-order kinetics, as shown in Figure 6. The second-order rate law was verified by changing the effective radical ion pair concentration by employing different laser power over a wide range (i.e., increments to reach a 5-fold increase in laser intensity) and also by changing the initial **Fc-ZnP-H$_2$P-C$_{60}$** concentration (i.e., $(2.0-20) \times 10^{-6}$ M). From the best fits *inter*molecular ET dynamics were calculated that are nearly diffusion controlled (PhCN, $5.4 \times 10^9\ M^{-1}\ s^{-1}$; DMF, $2.5 \times 10^9\ M^{-1}\ s^{-1}$). To the point that this analysis is correct a complementary investigation in a solvent with an even higher viscosity (DMF: $\eta = 0.924$ [$10^{-3}$ Pa s]) was deemed important, which led us to probe Triton X-100 ($\eta = 7.2$ [$10^{-3}$ Pa s]). Despite succeeding with respect to slowing-down the diffusion-

(36) Fukuzumi, S.; Mochizuki, S.; Tanaka, T. *Inorg. Chem.* **1989**, *28*, 2459.

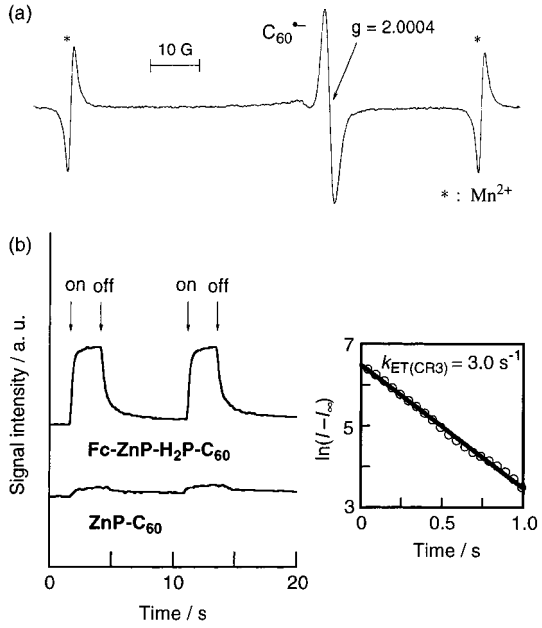


**Figure 7.** (a) ESR spectrum of **Fc-ZnP-H$_2$P-C$_{60}$** ($1.0 \times 10^{-5}$ M) in a frozen deaerated PhCN solution observed at 203 K under irradiation of ultraviolet−visible light from a high-pressure Hg lamp and (b) signal intensity response of **Fc-ZnP-H$_2$P-C$_{60}$** ($1.0 \times 10^{-5}$ M, top) and **ZnP-C$_{60}$** ($1.0 \times 10^{-5}$ M, bottom) in a frozen deaerated PhCN solution at the maximum of the ESR signal intensity due to the $C_{60}^{\bullet-}$. First-order plot for the decay of the ESR signal intensity ($I$) in **Fc-ZnP-H$_2$P-C$_{60}$** ($k_{ET(CR3)} = 3.0$ s$^{-1}$) is shown in the right panel.

controlled limit by 1 order of magnitude, we still obtained dynamics that were best fitted to an *inter*molecular process with an associated rate constant of $6.9 \times 10^8$ M$^{-1}$ s$^{-1}$. This confirms that the *intra*molecular ET in **Fc$^+$-ZnP-H$_2$P-C$_{60}^{\bullet-}$** ($k_{ET(CR3)} < 10^2$ s$^{-1}$) is indeed *too slow* to compete with the diffusion-limited *inter*molecular ET even in a highly viscous solvent (Table 2).

**Electron Spin Resonance Measurements under Irradiation.** To segregate the *inter*molecular ET from the *intra*molecular ET processes in **Fc$^+$-ZnP-H$_2$P-C$_{60}^{\bullet-}$**, electron spin resonance (ESR) measurements were performed in a frozen matrix at variable temperatures using a low concentration in PhCN ($1.0 \times 10^{-5}$ M) under irradiation. The ESR spectrum (Figure 7a) under irradiation at 203 K shows a characteristic broad signal attributable to $C_{60}^{\bullet-}$ ($g = 2.0004$).[37] $C_{60}^{\bullet-}$ was also produced via chemical reduction of **C$_{60}$-ref** (Figure 1) with tetramethylsemiquinone radical anion, yielding essentially an identical ESR signal. As far as direct ESR evidence for the ferricenium ion ($Fc^+$) in the **Fc$^+$-ZnP-H$_2$P-C$_{60}^{\bullet-}$** pair is concerned, its lack is rationalized in terms of well-known line-broadening of the $Fc^+$ ESR signal.[38]

The ESR signal was monitored at a fixed magnetic field to obtain maximal intensity of the $C_{60}^{\bullet-}$ response and to enable performance of the following lifetime experiments in frozen PhCN. As shown in Figure 7b, the ESR signal grows-in immediately upon "turning on" the irradiation of **Fc-ZnP-H$_2$P-C$_{60}$**. Only a slight amplification was noted during illumination. However, upon "turning off" the irradiation source, the ESR signal did not diminish instantly. Instead, it exhibited a slow and nearly seconds lasting decay, which was best fitted by first-order kinetics yielding a rate constant of 3.0 s$^{-1}$ (Figure 7b) for the *intra*molecular CR process ($k_{ET(CR3)}$). Furthermore, under similar experimental conditions, the ESR response of **Fc-ZnP-H$_2$P-C$_{60}$** was much larger than those of **ZnP-C$_{60}$** and **ZnP-H$_2$P-C$_{60}$** despite the lower quantum yield of CS for **Fc-ZnP-H$_2$P-C$_{60}$** (0.24) in PhCN solution relative to those of **ZnP-C$_{60}$** (0.85[22e]) and **ZnP-H$_2$P-C$_{60}$** (0.40[22e]). The latter exhibited multiexponential decay profiles (Figure 7b), which suggests the involvement of intermolecular ET in **ZnP-C$_{60}$** and **ZnP-H$_2$P-C$_{60}$**.

The clean monoexponential dynamics corroborate that the origin of the **Fc-ZnP-H$_2$P-C$_{60}$** ESR signal is indeed the *intra*molecular radical ion pair (**Fc$^+$-ZnP-H$_2$P-C$_{60}^{\bullet-}$**).[39] In contrast, an intermolecular ET, as it may prevail between radical ion pairs located in close proximity, should exhibit multiexponential decay profiles, depending on the relative distance between the radical ion pairs. Under the present experimental conditions this contribution was found to be negligible. To further test this hypothesis, the concentration was increased systematically up to $1.0 \times 10^{-4}$ M. In fact, at higher concentrations the first-order decay started to be mixed with a slower multiexponential decay due to the intermolecular ET.

The temperature dependence of $k_{ET(CR3)}$ reveals only a moderate change (2.6−3.0 s$^{-1}$) upon varying the temperature between 163 and 203 K. Similar results were obtained in DMF ($k_{ET(CR3)} = 2.9-3.4$ s$^{-1}$) within a range of 163−193 K. The weak temperature dependence suggests that a stepwise *intra*molecular CR process of **Fc$^+$-ZnP-H$_2$P-C$_{60}^{\bullet-}$** via a transient **Fc-ZnP$^{\bullet+}$-H$_2$P-C$_{60}^{\bullet-}$** intermediate can be ruled out with a high degree of confidence.

To analyze the ET reaction of **Fc-ZnP-H$_2$P-C$_{60}$** in light of the thermodynamic parameters, the following equations (eq 3 and 4) were employed:[1]

$$k_{ET} = \left(\frac{4\pi^3}{h^2 \lambda k_B T}\right)^{1/2} V^2 \exp\left[-\frac{(\Delta G^0_{ET} + \lambda)^2}{4\lambda k_B T}\right] \qquad (3)$$

$$\Delta G^{\#} = \frac{(\Delta G^0_{ET} + \lambda)^2}{4\lambda} \qquad (4)$$

with $\lambda$ being the reorganization energy, $\Delta G^0_{ET}$ the free energy change of ET, $V$ the electronic coupling matrix element, $T$ the absolute temperature, and $\Delta G^{\#}$ the activation barrier for the ET reaction. The "Marcus equation" (eq 3) was then transformed to its linear form as given in eq 5, which, in turn, enabled evaluation of $\Delta G^{\#}$, $\lambda$, and $V$.

$$\ln(k_{ET} T^{1/2}) = \ln\left(\frac{2\pi^{3/2} V^2}{h(\lambda k_B)^{1/2}}\right) - \frac{(\Delta G^0_{ET} + \lambda)^2}{4\lambda k_B T} \qquad (5)$$

The Arrhenius plots, that is, the ET rate ($k_{ET(CR3)}$) as a reciprocal function of the absolute temperature, reveal no appreciable deviation from the best-fitted straight line (Figure 8). Importantly, the small activation barriers ($\Delta G^{\#}$) of 0.012 and 0.016 eV in PhCN and DMF, respectively, infer that these

(37) Fukuzumi, S.; Mori, H.; Suenobu, T.; Imahori, H.; Gao, X.; Kadish, K. M. *J. Phys. Chem. A* **2000**, *104*, 10688.

(38) (**Fc-ref**)$^+$ produced by the oxidation with $Ru(bpy)_3^{3+}$ (bpy = 2,2′-bipyridine) exhibits no significant ESR signal under the same experimental conditions.

(39) Gust et al.[15h] reported that freebase porphyrin−$C_{60}$ dyad reveals photoinduced ET from the porphyrin excited singlet state to the $C_{60}$ even in the rigid glass down to at least 8 K. They suggested that the energy of the $C_{60}$ radical anion was less sensitive to solvents effect than that of semiquinone radical anion, as the $C_{60}$ radical anion is a relatively large, spherical ion having the charge spread over the three-dimensional carbon framework. Thus, destabilization of the $C_{60}$ radical anion by frozen solvents should be mimimal. The unique behavior was rationalized by our proposal that fullerenes have small reorganization energies in ET.[13,14] Overall, the **Fc-ZnP-H$_2$P$^{\bullet+}$-C$_{60}^{\bullet-}$** state may be less destabilized even in frozen benzonitrile or DMF, thereby leading to the production of the final charge-separated state (**Fc$^+$-ZnP-H$_2$P-C$_{60}^{\bullet-}$**).

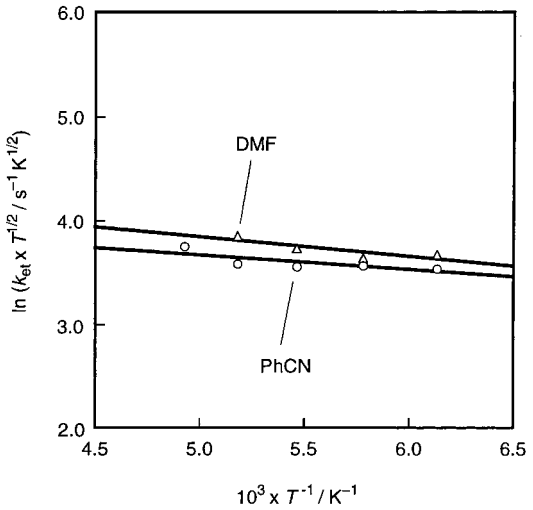


**Figure 8.** Arrhenius analyses of the temperature-dependent ET rate constants ($k_{ET(CR3)}$) for **Fc-ZnP-H$_2$P-C$_{60}$** in frozen PhCN (circles) and DMF (triangles). The Arrhenius plots of the ET rates against the reciprocal of absolute temperature gave a straight line with the intercept (PhCN, 4.38; DMF, 4.80) and the slope (PhCN, 0.142; DMF, 0.191) according to eq 5.

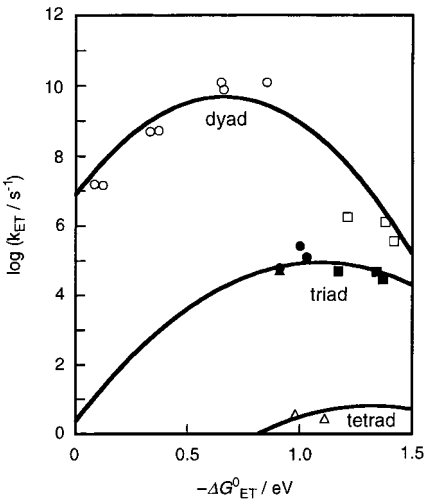


**Figure 9.** Driving force ($-\Delta G^0_{ET}$) dependence of intramolecular ET rate constants in **ZnP-C$_{60}$** (CS, open circles; CR, open squares), **Fc-ZnP-C$_{60}$** (solid circles), **Fc-H$_2$P-C$_{60}$** (solid triangles), **ZnP-H$_2$P-C$_{60}$** (solid squares), and **Fc-ZnP-H$_2$P-C$_{60}$** (open triangles). The lines represent the best fit to eq 3 (**ZnP-C$_{60}$**, $\lambda = 0.66$ eV, $V = 3.9$ cm$^{-1}$, [22f]; **Fc-ZnP-C$_{60}$**, **Fc-H$_2$P-C$_{60}$**, and **ZnP-H$_2$P-C$_{60}$**, $\lambda = 1.09$ eV, $V = 0.019$ cm$^{-1}$, [22f]; **Fc-ZnP-H$_2$P-C$_{60}$**, $\lambda = 1.32$ eV, $V = 0.00017$ cm$^{-1}$).

ET processes occur in the top region of the "Marcus curve" to give the optimal rate constant ($k_{ET(optimal)}$) (Figure 9). From a closer inspection of the Arrhenius plots, the reorganization energy ($\lambda$) and the electronic coupling matrix element ($V$) were determined as 1.37 eV in PhCN and 1.27 eV in DMF and 1.6 $\times$ $10^{-4}$ cm$^{-1}$ in PhCN, and 1.9 $\times$ $10^{-4}$ cm$^{-1}$ in DMF, respectively.

Finally, to shed light onto the *intra*molecular ET process, the $k_{ET(optimal)}$ values of **Fc-ZnP-H$_2$P-C$_{60}$** ($R_{ee} = 48.9$ Å), **Fc-ZnP-C$_{60}$**, **Fc-H$_2$P-C$_{60}$**, **ZnP-H$_2$P-C$_{60}$** ($R_{ee} = 30.3$ Å), and **ZnP-C$_{60}$** ($R_{ee} = 11.9$ Å) (Table 3 and Figure 9) are correlated with the edge-to-edge distance ($R_{ee}$), separating the radical ions, according to eq 6 and 7:

$$k_{ET(optimal)} = \left(\frac{4\pi^3}{h^2\lambda k_B T}\right)^{1/2} V^2 = \left(\frac{4\pi^3}{h^2\lambda k_B T}\right)^{1/2} V_0^{\,2} \exp(-\beta R_{ee}) \quad (6)$$

$$\ln(k_{ET}(optimal)) = \ln\left(\frac{2\pi^{3/2} V_0^{\,2}}{h(\lambda k_B T)^{1/2}}\right) - \beta R_{ee} \quad (7)$$

Hereby, $V_0$ refers to the maximal electronic coupling element, while $\beta$ is the decay coefficient factor (damping factor), which depends primarily on the nature of the bridging molecule. The plots are fitted well with a straight line, including the extremely slow CR process of **Fc-ZnP-H$_2$P-C$_{60}$** tetrad to yield $V_0 = 210$ cm$^{-1}$ and $\beta = 0.60$ Å$^{-1}$ (Figure 10). This $\beta$ value is located within the boundaries of nonadiabatic ET reactions for saturated hydrocarbon bridges (0.8−1.0 Å$^{-1}$) and unsaturated phenylene bridges (0.4 Å$^{-1}$).[1,40]

In summary, the present study has demonstrated unequivocally occurrence of an *intra*molecular CR process in the **Fc-ZnP-H$_2$P-C$_{60}$** tetrad, observable by ESR measurements under irradiation. More importantly, the lifetimes (0.38 s in PhCN at 193 K and 0.34 s in DMF at 173 K) are by far the longest values ever reported for *intra*molecular CR in a donor−acceptor ensemble (with earlier values at 340 $\mu$s in solutions[24] and 12.7 ms at 77 K[25]). They are also comparable, for example, to the

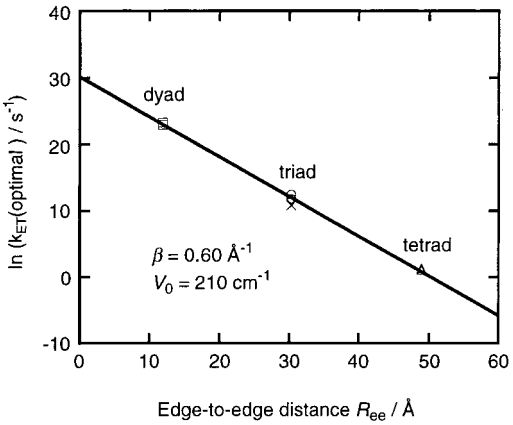


**Figure 10.** Edge-to-edge distance ($R_{ee}$) dependence of optimal electron-transfer rate constants (ln[$k_{ET}$(optimal)/s$^{-1}$]) in **ZnP-C$_{60}$** dyad (square), **Fc-ZnP-C$_{60}$** triad (circle), **Fc-H$_2$P-C$_{60}$** triad (diamond), **ZnP-H$_2$P-C$_{60}$** triad (cross), and **Fc-ZnP-H$_2$P-C$_{60}$** tetrad (triangle). The line represents the best fit to eq 7 ($\beta = 0.60$ Å$^{-1}$, $V_0 = 210$ cm$^{-1}$).

lifetimes ($\sim$1 s$^{-1}$) of the bacteriochlorophyll dimer radical cation ((Bchl)$_2^{\bullet+}$)−secondary quinone radical anion ($Q_B^{\bullet-}$) ion pair in the bacteria photosynthetic reaction centers.[11] Such an extremely long lifetime of a CS state could only be determined in frozen media, since in condensed media *inter*molecular dynamics dominate the back ET. It should also be emphasized that such an extremely long lifetime of the tetrad system has been well correlated with the charge-separated lifetimes of two homologous series of porphyrin−fullerene dyad and triad systems.

## Experimental Section

**General.** Melting points were recorded on a Yanagimoto micro-melting point apparatus and not corrected. $^1$H NMR spectra were measured on a JEOL EX-270 or a JEOL JNM-LA400. Fast atom bombardment mass spectra (FABMS) were obtained on a JEOL JMS-DX300. Matrix-assisted laser desorption/ionization (MALDI) time-of-flight (TOF) mass spectra were measured on a Kratos Compact MALDI I (Shimadzu). IR spectra were measured on a Perkin-Elmer FT-IR 2000 spectrophotometer as KBr disks. Steady-state absorption spectra were

(40) Helms, A.; Heiler, D.; McLendon, G. *J. Am. Chem. Soc.* **1992**, *114*, 6227.

measured on a Shimadzu UV3000 spectrometer. Elemental analyses were performed on a Perkin-Elmer Model 240C elemental analyzer. The edge-to-edge distances ($R_{ee}$) were determined from CPK modeling using CAChe (version 3.7 CAChe Scientific, 1994).

**Materials.** All solvents and chemicals were of reagent grade quality, obtained commercially and used without further purification except as noted below. Tetrabutylammonium hexafluorophosphate used as a supporting electrolyte for the electrochemical measurements was obtained from Tokyo Kasei Organic Chemicals. THF, benzonitrile, and DMF were purchased from Wako Pure Chemical Ind., Ltd., and purified by successive distillation over calcium hydride. Thin-layer chromatography (TLC) and flash column chromatography were performed with Art. 5554 DC-Alufolien Kieselgel 60 $F_{254}$ (Merck) and Fujisilicia BW300, respectively.

**Synthesis of Tetrads. 2**: A solution of dipyrromethane **1**[27] (15.62 g, 58.44 mmol) and 3,5-di-*tert*-butylbenzaldehyde[28] (12.76 g, 58.44 mmol) in chloroform (4000 mL) was degassed by bubbling with nitrogen for 1 h. The reaction vessel was shielded from ambient light. Then boron trifluoride diethyl etherate (7.43 mL, 58.6 mmol) was added at one portion. The solution was stirred for 2 h at room temperature under nitrogen atmosphere. To the reddish black reaction mixture was added *p*-chloranil (21.55 g, 87.64 mmol) with overnight stirring. Triethylamine (25.2 mL, 181 mmol) was added and then the reaction mixture was concentrated. Flash column chromatography on silica gel with chloroform as the eluent gave a mixture of several porphyrins. Subsequent flash column chromatography on silica gel (toluene) yielded the desired porphyrin from the mixture as the third major band. Reprecipitation with chloroform−methanol afforded **2** as a vivid reddish purple solid (3.14 g, 3.38 mmol, 12% yield). Mp >300 °C; $^1$H NMR (270 MHz, $CDCl_3$) $\delta$ −2.75 (br s, 2H), 1.53 (s, 36H), 7.82 (t, $J$ = 2 Hz, 2H), 8.08 (d, $J$ = 2 Hz, 4H), 8.41 (d, $J$ = 8 Hz, 4H), 8.64 (d, $J$ = 8 Hz, 4H), 8.75 (d, $J$ = 5 Hz, 4H), 8.95 (d, $J$ = 5 Hz, 4H); FABMS *m*/*z* 929 (M + H$^+$).

**3:** To a suspension of **2** (201 mg, 0.217 mmol) in concentrated HCl solution (50 mL) was added $SnCl_2$ (276 mg, 1.46 mmol). The reaction mixture was stirred for 45 min at room temperature and maintained at 95−100 °C for an additional 30 min. After cooling, the reaction was quenched by the slow addition of 25% ammonia solution. The organic layer was extracted with $CHCl_3$ and washed with water. After standing over anhydrous $Na_2SO_4$, the organic extract was concentrated to dryness. Flash column chromatography on silica gel with toluene−ethyl acetate (30:1) as the eluent and subsequent reprecipitation from $CHCl_3$−$CH_3CN$ gave **3** as a deep violet solid (123 mg, 0.142 mmol, 65%). Mp >300 °C; $^1$H NMR (270 MHz, $CDCl_3$) $\delta$ −2.71 (br s, 2H), 1.53 (s, 36H), 4.02 (br s, 4H), 7.06 (d, $J$ = 8 Hz, 4H), 7.79 (t, $J$ = 2 Hz, 2H), 8.00 (d, $J$ = 8 Hz, 4H), 8.08 (d, $J$ = 2 Hz, 4H), 8.87 (d, $J$ = 5 Hz, 4H), 8.92 (d, $J$ = 5 Hz, 4H); FABMS *m*/*z* 869 (M + H$^+$).

**4**: Oxalyl chloride (0.190 mL, 2.18 mmol) was added to a stirred solution of sodium 4-ferrocenylbenzoate[29] (70.5 mg, 0.215 mmol) in dry $CH_2Cl_2$ (15 mL) and pyridine (0.01 mL). The resulting solution was stirred for 13 h at room temperature and then refluxed for 5 h. Excess oxalyl chloride and solvents were removed under reduced pressure and the residue was redissolved in dry toluene (20 mL). This solution was added to a stirred solution of **3** (373 mg, 0.430 mmol) and pyridine (6.0 mL) in dry toluene (150 mL), and the solution was stirred for 18 h. The reaction mixture was evaporated. Flash column chromatography on silica gel with toluene−ethyl acetate (80:1) as the eluent and subsequent reprecipitation from $CHCl_3$−$CH_3CN$ gave a deep violet solid. A saturated methanol solution of $Zn(OAc)_2$ (5.0 mL) was added to a solution of the deep violet solid in $CHCl_3$ (50 mL) and refluxed for 30 min. After cooling, the reaction mixture was washed with water twice and dried over anhydrous $Na_2SO_4$, and then the solvent was evaporated. Flash column chromatography on silica gel with $CHCl_3$ as an eluent and subsequent reprecipitation from chloroform−methanol gave **4** as a deep violet solid (113 mg, 0.0926 mol, 43% yield). Mp >300 °C; $^1$H NMR (270 MHz, $CDCl_3$ + pyridine-$d_5$) $\delta$ 1.52 (s, 36H), 4.08 (s, 5H), 4.41 (t, $J$ = 2 Hz, 2H), 4.75 (t, $J$ = 2 Hz, 2H), 7.03 (d, $J$ = 8 Hz, 2H), 7.61 (d, $J$ = 8 Hz, 2H), 7.77 (t, $J$ = 2 Hz, 2H), 7.98 (d, $J$ = 8 Hz, 2H), 7.99 (d, $J$ = 8 Hz, 2H), 8.05 (d, $J$ = 8 Hz, 2H), 8.06 (d, $J$ = 2 Hz, 4H), 8.21 (d, $J$ = 8 Hz, 2H), 8.91 (d, $J$ = 5 Hz, 2H), 8.92 (s, 4H), 8.97 (d, $J$ = 5 Hz, 2H); FABMS *m*/*z* 1221 (M + H$^+$).

**6**: A solution of **5**[22e] (153 mg, 0.165 mmol), thionyl chloride (0.370 mL, 5.07 mmol), and pyridine (0.20 mL) in benzene (30.0 mL) was refluxed for 2 h under nitrogen atmosphere. Excess reagent and solvents were removed under reduced pressure, and the residue was redissolved in a mixture of toluene (20 mL) and pyridine (1.0 mL). To the reaction mixture were added a solution of **4** (99.8 mg, 0.0818 mmol) and 4-*tert*-butyldimethylsilyloxymethylaniline[22e] (60.8 mg, 0.256 mmol) in toluene (30.0 mL) and pyridine (1.0 mL). The solution was allowed to stir overnight at room temperature under nitrogen atmosphere. TLC showed three products ($R_f$ = 0.60, 0.45, and 0.40, benzene/ethyl acetate = 9/1) and the second band was separated by flash column chromatography on silica gel (chloroform/triethylamine = 100/0.25) and subsequent reprecipitation from benzene−$CH_3CN$ gave a deep violet solid. To a solution of the deep violet solid in THF (40 mL) was added 0.640 mL of tetrabutylammonium fluoride (1 M in THF), then the mixture was stirred for 3.5 h at room temperature under nitrogen atmosphere. The solvents were removed under reduced pressure. Flash column chromatography on silica gel (toluene/ethyl acetate = 9/1) and subsequent reprecipitation from chloroform−acetonitrile afforded **6** as a deep purple solid (74.9 mg, 0.0335 mmol, 41% yield). Mp >300 °C; $^1$H NMR (400 MHz, $CDCl_3$; some of the signals could not be assigned because of the poor solubility) $\delta$ −2.68 (br s, 2H), 1.56 (s, 72H), 4.11 (s, 5H), 4.45 (s, 2H), 4.68 (d, $J$ = 5 Hz, 2H), 4.79 (s, 2H), 7.5−9.1 (m, 55 H); MALDI-TOFMS (positive mode) *m*/*z* 2236 (M + H$^+$).

**7**: To a solution of **6** (39.9 mg, 0.0179 mol) in chloroform (65 mL) was added activated manganese dioxide (398 mg) in one portion, and then the suspended mixture was stirred for 3.5 h at room temperature under nitrogen atmosphere. The catalyst was removed by filtration and the filtrate was concentrated under reduced pressure. Flash column chromatography on silica gel (benzene/ethyl acetate = 9/1) and subsequent reprecipitation from chloroform−acetonitrile afforded **7** as a deep purple solid (30.9 mg, 0.0138 mmol, 77% yield). Mp >300 °C; $^1$H NMR (270 MHz, $CDCl_3$) $\delta$ −2.67 (br s, 2H), 1.55 (s, 72H), 4.10 (s, 5H), 4.44 (s, 2H), 4.77 (s, 2H), 7.64 (s, 2H), 7.8−8.5 (m, 37H), 8.7−9.2 (m, 16H), 9.98 (s, 1H); MALDI-TOFMS (positive mode) *m*/*z* 2234 (M + H$^+$).

**Fc-ZnP-$H_2$P-$C_{60}$**: A solution of **7** (17.2 mg, 0.00770 mmol), $C_{60}$ (27.8 mg, 0.0386 mmol), and *N*-methylglycine (35.1 mg, 0.394 mmol) in toluene (40 mL) was refluxed under nitrogen atmosphere until TLC analysis showed no detection of **7**. The reaction mixture was poured on the top of a flash chromatography column (silica gel) that was washed with toluene as an eluate to remove unreacted $C_{60}$. Then the column was washed with chloroform, eluting the desired product. Reprecipitation from chloroform−methanol afforded **Fc-ZnP-$H_2$P-$C_{60}$** as a dark violet solid (13.3 mg, 0.00446 mmol, 58% yield). Mp >300 °C; $^1$H NMR (400 MHz, $CDCl_2CDCl_2$, 60 °C) $\delta$ −2.65 (s, 2H), 1.57 (s, 36H), 1.59 (s, 36H), 2.86 (s, 3H), 4.13 (s, 5H), 4.20 (d, $J$ = 10 Hz, 1H), 4.46 (s, 2H), 4.79 (s, 2H), 4.90 (s, 1H), 4.94 (d, $J$ = 10 Hz, 1H), 7.68 (d, $J$ = 8 Hz, 2H), 7.84 (t, $J$ = 2 Hz, 4H), 7.90 (s, 4H), 7.98 (d, $J$ = 8 Hz, 2H), 8.07 (d, $J$ = 8 Hz, 2H), 8.11 (d, $J$ = 2H, 4H), 8.14 (d, $J$ = 2 Hz, 4H), 8.17 (br s, 1H), 8.22 (d, $J$ = 8 Hz, 2H), 8.26 (d, $J$ = 8 Hz, 2H), 8.28 (br s, 1H), 8.30 (d, $J$ = 8 Hz, 2H), 8.36 (d, $J$ = 8 Hz, 2H), 8.38 (d, $J$ = 8 Hz, 2H), 8.45 (d, $J$ = 8 Hz, 2H), 8.50 (d, $J$ = 8 Hz, 2H), 8.52 (br s, 1H), 8.83 (d, $J$ = 5 Hz, 2H), 8.92 (d, $J$ = 5 Hz, 2H), 8.96 (d, $J$ = 5 Hz, 2H), 8.99 (d, $J$ = 5 Hz, 2H), 9.05 (d, $J$ = 5 Hz, 2H), 9.07 (d, $J$ = 5 Hz, 2H), 9.10 (d, $J$ = 5 Hz, 2H), 9.12 (d, $J$ = 5 Hz, 2H); MALDI-TOFMS (positive mode) *m*/*z* 2981 (M + H$^+$), 2260 [M − $C_{60}$]$^+$; UV−vis (PhCN) $\lambda_{max}$ (log $\epsilon$) 432 (5.91), 519 (4.40), 557 (4.52), 600 (4.22), 650 (3.78).

**Fc-ref:** Oxalyl chloride (1.0 mL, 11 mmol) was added to a stirred solution of sodium 4-ferrocenylbenzoate (0.600 g, 1.83 mmol)[29] in dry $CH_2Cl_2$ (50 mL) and pyridine (0.1 mL). The resultant solution was stirred for 14 h at room temperature and then refluxed for 5 h. The excess oxalyl chloride and solvents were removed under a reduced pressure and the residue was redissolved in dry $CH_2Cl_2$ (25 mL). This solution was added to a stirred solution of aniline (1.0 mL, 11 mmol) in dry $CH_2Cl_2$ (25 mL) and then stirred for 28 h. The reaction mixture was poured into 150 mL of water, extracted with $CHCl_3$, dried over anhydrous $Na_2SO_4$, and evaporated. Recrystallization from tol-

uene gave **Fc-ref** as orange needles (0.580 g, 1.52 mmol, 83%). $^1$H NMR (270 MHz, $CDCl_3$) $\delta$ 7.80 (d, $J = 8$ Hz, 2H), 7.79 (s, 1H), 7.66 (d, $J = 8$ Hz, 2H), 7.57 (d, $J = 8$ Hz, 2H), 7.39 (t, $J = 8$ Hz, 2H), 7.16 (t, $J = 8$ Hz, 1H), 4.72 (t, $J = 2$ Hz, 2H), 4.40 (t, $J = 2$ Hz, 2H), 4.05 (s, 5H); MS (FAB) 382 ($M + H^+$); UV−vis ($CH_2Cl_2$) $\lambda_{max}$ (log $\epsilon$) 263 (4.22), 300 (4.37), 362 (3.52), 455 (3.04). Anal. Calcd for $C_{23}H_{19}FeNO$: C, 72.46; H, 5.02; N, 3.67. Found: C, 72.73; H, 4.83; N, 3.68.

**Flash Photolysis Experiments.** For flash-photolysis studies, the fullerene concentrations were prepared to exhibit an optical density of at least 0.02 at 532 nm, the wavelength of irradiation. Picosecond laser flash photolysis experiments were carried out with 532-nm laser pulses from a mode-locked, *Q*-switched Quantel YG-501 DP ND:YAG laser system (pulse width $\sim$ 18 ps, 2−3 mJ/pulse).[22e] The white continuum picosecond probe pulse was generated by passing the fundamental output through a $D_2O/H_2O$ solution. Nano- to millisecond laser flash photolysis experiments were performed with laser pulses from a Qunta-Ray CDR Nd:YAG system (532 nm, 6 ns pulse width) in a front face excitation geometry.[22e] A Xe lamp was triggered synchronously with the laser. A monochromator (SPEX) in combination with either a Hamamatsu R 5108 photomultiplier or a fast InGaAs-diode was employed to monitor transient absorption spectra. The quantum yields were measured using the comparative method.[22e] In particular, the strong fullerene triplet−triplet absorption ($\epsilon_{700\ nm} = 16100\ M^{-1}\ cm^{-1}$; $\Phi_{TRIPLET} = 0.98$)[22e] served as probe to obtain the quantum yields for the CS state, especially for the fullerene $\pi$-radical anion ($\epsilon_{1000\ nm} = 4700\ M^{-1}\ cm^{-1}$).[22e]

**ESR Measurements under Photoirradiation.** A quartz ESR tube (internal diameter: 4.5-mm) containing a deaerated PhCN solution of porphyrin−fullerene linked compounds ($1.0 \times 10^{-5}$ M) was irradiated in the cavity of the ESR spectrometer with the focused light of a 1000-W high-pressure Hg lamp (Ushio-USH1005D) through an aqueous filter. The internal diameter of the ESR tube is 4.5 mm, which is small enough to fill the ESR cavity but large enough to obtain good signal-to-noise ratios during the ESR measurements under photoirradiation at low temperatures. The ESR spectra in frozen PhCN or DMF were measured under nonsaturating microwave power conditions at various temperatures (163 to 203 K) with a JEOL X-band spectrometer (JES-RE1XE) using an attached variable-temperature apparatus.

**Acknowledgment.** This work was supported by Grant-in-Aids for COE Research and Scientific Research on Priority Area of Electrochemistry of Ordered Interfaces and Creation of Delocalized Electronic Systems from the Ministry of Education, Culture, Sports, Science and Technology, Japan, a Millennium Project from the Science and Technology Agency, Japan (No. 12310), and the Office of Basic Energy Sciences of the U.S. Department of Energy, U.S.A. H.I. thanks the Sumitomo Foundation for financial support. This is document NDRL-4273 from the Notre Dame Radiation Laboratory.

JA004123V